Pulsed Laser Photolysis and Thermodynamics Studies of Intramolecular Electron Transfer in Valence Tautomeric Cobalt *o*-Quinone Complexes

David M. Adams and David N. Hendrickson*

Contribution from the Department of Chemistry and Biochemistry-0358, University of California at San Diego, La Jolla, California 92093-0358

Received June 10, 1996[⊗]

Abstract: Four valence tautomeric complexes with the general composition [Co(3,5-DTBSQ)$_2$(N⌒N)] have been investigated, where 3,5-DTBSQ$^-$ is the semiquinonate form of 3,5-di-*tert*-butyl-*o*-quinone. The diiminium ligand N⌒N is one of the following ligands: phen (1,10-phenanthroline, complex **1**); bpy (2,2′-bipyridine, complex **2**); dmbpy (4,4′-dimethyl-2,2′-bipyridine, complex **3**); dpbpy (4,4′-diphenyl-2,2′-bipyridine, complex **4**). All four of the complexes undergo a valence tautomerism converting from low-spin (ls) [Co^{III}(3,5-DTBSQ)(3,5-DTBCAT)(N⌒N)] at low temperatures to high-spin (hs) [Co^{II}(3,5-DTBSQ)$_2$(N⌒N)] at high temperatures, where the 3,5-DTBCAT^{2-} ligand is the catecholate form of the *o*-quinone ligand. Variable temperature (150−340 K) magnetic susceptibility data are presented for toluene solutions of all four complexes. These data were least-squares fit to give ΔH and ΔS values that characterize the valence tautomerism equilibrium. The ΔH values range from 21.33 to 38.36 kJ mol^{-1}, whereas the ΔS values range from 60.6 to 133.8 J mol^{-1} K^{-1}. Analogous to Fe^{II} spin crossover complexes, the cobalt valence tautomerism is an entropy driven process. Electronic and vibrational (changes in metal−ligand and ligand-based vibrations) entropy contributions are present that drive the ls-[Co^{III}(SQ)(Cat)] to hs-[Co^{II}(SQ)$_2$] conversion when the temperature is increased. Variable temperature electronic absorption spectra (320−820 nm) are presented for the complexes in toluene solution and for polystyrene-doped samples. The presence of isosbestic points indicates only two species are present. Optical spectra show that, compared to the situation in toluene solution, doping the cobalt tautomeric complexes into polystyrene leads to stabilization of the smaller ls-Co^{III} tautomer. Pulsed laser photolysis, both on the picosecond (90 ps pulse) and the nanosecond (24 ns pulse) time scales, were carried out for solutions of the complexes. The laser pulse into the 600 nm band of the ls-Co^{III} tautomer excites the complex to a ligand to metal charge transfer (LMCT) excited state. Some molecules rapidly intersystem cross to the hs-Co^{II} state. The rate of back valence tautomerization, k_{bvt}, for conversion from the hs-Co^{II} to the ls-Co^{III} state can be measured. At room temperature in toluene solution, k_{bvt} was determined with picosecond spectroscopy to be 6.08×10^7 s^{-1} for complex **3** and 6.71×10^8 s^{-1} for complex **4**. Since no indication of a rise time was seen, the hs-Co^{II} state is formed within the experimental resolution of 90 ps. The observation of a bleach and an absorption with identical kinetics when the probe wavelength is moved to either side of an isosbestic point confirms that the hs-Co^{II} to ls-Co^{III} conversion is being monitored. Nanosecond laser spectroscopy was used to determine the temperature dependence of k_{bvt}. For complex **4** in 2-methyltetrahydrofuran, data were collected in the 110.5−198.1 K range. There is evidence of a change from an Arrhenius-type behavior to a temperature-independent rate below ∼132 K. The quantum mechanical theory of radiationless transitions of Buhks and Jortner was used to fit the temperature dependence of k_{bvt}. It appears the hs-Co^{II} to ls-Co^{III} valence tautomerism may occur by quantum mechanical tunneling.

Introduction

Redox active organic ligands complexed to redox active metal ions can lead to molecules that exhibit valence tautomerism. Transition metal complexes of Co,[1−3] Mn,[4] Fe,[5] Rh and Ir,[6] and Cu[7] with ligands derived from *o*-benzoquinone have been shown to exhibit valence tautomerism. Valence tautomers are characterized by different distributions of electron density, where interconversion between tautomers is accomplished by intramolecular electron transfer. There are two important reasons for studying valence tautomeric complexes. First, they are unique model systems which provide insight into the factors that affect intramolecular electron transfer in coordination complexes. Second, from an applied perspective, the large changes in the optical, structural, and magnetic properties that often accompany the valence tautomeric interconversion have potential applications in bistable molecular level switching materials.[8]

Complexes that exhibit valence tautomerism are electronically labile, where two or more electronic states lie close in energy, and this leads to significant vibronic interactions and an

[⊗] Abstract published in *Advance ACS Abstracts,* November 1, 1996.

(1) (a) Adams, D. M.; Dei, A.; Rheingold, A. L; Hendrickson, D. N. *Angew. Chem., Int. Ed. Engl.* **1993**, *32*, 880. (b) Adams, D. M.; Dei, A.; Rheingold, A. L.; Hendrickson, D. N. *J. Am. Chem. Soc.* **1993**, *115*, 8221.

(2) Abakumov, G. A.; Cherkasov, V. K.; Bubnov M. P.; Ellert, O. G.; Dobrokhotova, Z. B.; Zarkharov, L. N.; Struchovkov,Y. T. *Dokl. Akad. Nauk.* **1993**, *328*, 12.

(3) (a) Buchanan, R. M.; Pierpont, C. G. *J. Am. Chem. Soc.* **1980**, *102*, 4951. (b) Jung, O. S.; Pierpont, C. G. *Inorg. Chem.* **1994**, *33*, 2227.

(4) (a) Lynch, M. W.; Hendrickson, D. N.; Fitzgerald, B. J.; Pierpont, C. G. *J. Am. Chem. Soc.* **1984**, *106*, 2041. (b) Attia, S. A.; Pierpont, C. G. *Inorg. Chem.* **1995**, *34*, 1172.

(5) (a) Lynch, M. W.; Valentine, M.; Hendrickson, D. N. *J. Am. Chem. Soc.* **1982**, *104*, 6982. (b) Attia, S. A.; Bhattacharya, S.; Pierpont, C. G. *Inorg. Chem.* **1995**, *34*, 4427. (c) Attia, A. S.; Jung, O. S.; Pierpont, C. G. *Inorg. Chim. Acta* **1994**, *226*, 91.

(6) Abakumov, G. A.; Razuvaev, G. A.; Nevodchikov, V. I.; Cherkasov, V. K. *J. Organomet. Chem.* **1988**, *341*, 485.

(7) Abakumov, G. A.; Garnov, V. A.; Nevodchikov, V. I.; Cherkasov, V. K *Dokl. Akad. Nauk. SSSR* **1989**, *304*, 107.

(8) Hendrickson, D. N.; Adams, D. M.; Wu, C. C. In *Magnetism: A Supramolecular Function*; Kahn, O., Ed.; NATO ASI Series; Kluwer Publishing Co.: Dordrecht, The Netherlands. In press.

S0002-7863(96)01956-7 CCC: $12.00

appreciable sensitivity to the environment. Other examples of electronic lability are found in mixed valence[9] and spin crossover[10] complexes. Electronically labile complexes are potential building blocks for molecular electronic devices.[11] An external perturbation (e.g., photons, electric field, magnetic field, etc.) on small collections of these molecules can lead to an interconversion between two electronic states. In fact, Gütlich et al.[12] have shown that polycrystalline samples of Fe^{II} spin crossover complexes maintained at low temperatures (<50 K) can be reversibly interconverted between the *low-spin* and a long-lived metastable *high-spin* state in the LIESST (light-induced excited spin state trapping) effect. Recently, Kahn et al.[13] have been able to prepare Fe^{II} spin crossover complexes in which the bulk samples display large hysteresis loops centered around room temperature. A display device has been fabricated where images can be switched between the purple (low-spin, ls) and white (high-spin, hs) colored forms of the complex. Hauser[14] also showed that Fe^{II} spin crossover complexes exhibit a large photorefractive effect between the *low-spin* and *high-spin* forms of Fe^{II}. He was able to induce dynamic as well as static holographic grating formation, the decay of which could be modulated by the temperature. This behavior is attractive for real-time holography applications.

In our laboratory, we have been concerned with understanding and controlling the cobalt bis-*o*-quinone valence tautomeric interconversion. Cobalt complexes with two *o*-quinone derived ligands have been shown to undergo a valence tautomeric interconversion between *high-spin*-[$Co^{II}(SQ)_2(N\frown N)$] and *low-spin*-[$Co^{III}(SQ)(CAT)(N\frown N)$], where$N\frown N$ is a chelating nitrogen donor ligand such as 2,2-bipyridine (bpy) and SQ^- and CAT^{2-} refer, respectively, to the singly and doubly reduced forms of a substituted *o*-benzoquinone ligand. In these molecules an intramolecular electron transfer converts the *high-spin* Co^{II} into a *low-spin* Co^{III} ion, and one of the ligands is reduced by one electron from a semiquinone anion (SQ^-) to a catecholate (CAT^{2-}) ligand. There are two different mixed valence isomers of the ls-Co^{III} valence tautomer. The dynamical processes that are possible for such a valence tautomeric complex are summarized in Scheme 1.

Scheme 1. Possible Intramolecular Electron Transfer Processes Present for a Valence Tautomeric Cobalt Complex[a]

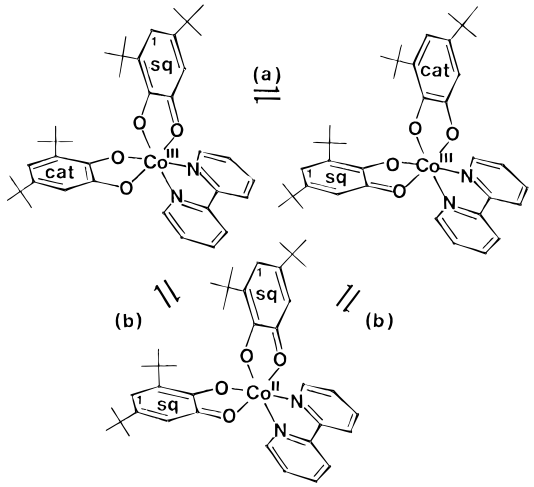

[a] Mixed valence process (a) involves transfer of an electron from CAT^{2-} π^* to the SQ^- π^* orbital. Valence tautomerism process (b) involves transfer of an electron from the CAT^{2-} π^* orbital to the low-spin Co^{III} ion in the forward direction and from the high-spin Co^{II} ion to the SQ^- π^* orbital in the reverse direction.

The valence tautomeric interconversion (process b) can be thermally driven. Initially, it was observed that the bipyridine complex in Scheme 1 could exist in the ls-Co^{III} and hs-Co^{II} valence tautomeric forms in solution.[3a] In toluene at room temperature, the hs-Co^{II} tautomer predominates. A decrease in temperature leads to a stabilization of the ls-Co^{III} tautomer such that at temperatures below ~250 K the ls-Co^{III} form predominates. Later we showed[1] that by changing the nitrogen donor ligand we could systematically shift the solution critical temperature ($T_{1/2}$) of the interconversion. This shift was attributed to a subtle modulation of the energy difference between valence tautomers by the counterligand. Furthermore, it was established that valence tautomerism can be thermally induced in the solid state.[1] It was shown that the ls-[Co^{III}(3,5-DTBSQ)(3,5-DTBCAT)(phen)]·$C_6H_5CH_3$ to hs-[Co^{II}(3,5-DTBSQ)$_2$ (phen)]·$C_6H_5CH_3$ interconversion can be reversibly driven with temperature and that the interconversion occurs abruptly within a narrow temperature range of ~30°. Recently, we have shown that the interconversion can be pressure induced[15] in the solid state and photoinduced[16] in solution and polymer films.

The observation that pulsed laser excitation can be used to photoinduce valence tautomerism is significant for it allows monitoring of intramolecular electron transfer kinetics in these systems. Time-resolved pulsed laser spectroscopy can be used to monitor the rate of back valence tautomerization (k_{bvt}) as given in eq 1:

$$\text{ls-}[Co^{III}(SQ)(CAT)(N\frown N)] \underset{k_{bvt}}{\overset{h\nu}{\rightleftharpoons}} \text{hs-}[Co^{II}(SQ)_2(N\frown N)] \qquad (1)$$

The valence tautomeric process is similar to the hs-Fe^{II} to ls-Fe^{II} spin crossover interconversion. The kinetics of Fe^{II} spin crossover have been shown to be largely modulated by appreciable Franck−Condon reorganization energies and energy differences between the *high-spin* and *low-spin* states.[17] Metal−

(9) (a) Day, P. *Int. Rev. Phys. Chem.* **1981**, *1*, 149. (b) Creutz, C. *Prog. Inorg. Chem.* **1983**, *30*, 1. (c) Richardson, D. E.; Taube, H. *Coord. Chem. Rev.* **1984**, *60*, 107. (d) Hendrickson, D. N. In *Mixed Valence Systems: Applications in Chemistry, Physics, and Biology*; Prassides, K., Ed.; NATO ASI Series; Kluwer Publishing Co.: Dordrecht, The Netherlands, 1991; pp 67−90.

(10) (a) Beattie, J. K. *Adv. Inorg. Chem.* **1988**, *32*, 1−53. (b) Konig, E. *Prog. Inorg. Chem.* **1987**, *35*, 527−622. (c) Rao, C. N. R. *Int. Rev. Phys. Chem.* **1985**, *4*, 19. (d) Gutlich, P. *Struct. Bonding (Berlin)* **1981**, *44*, 83. (e) Bacci, M. *Coord. Chem. Rev.* **1988**, *86*, 245. (f) Maeda, Y.; Takashima, Y. *Comments Inorg. Chem.* **1988**, *7*, 41. (g) Toftlund, H. *Coord. Chem. Rev.* **1989**, *94*, 67−108. (h) Zarembowitch, J. *New J. Chem.* **1992**, *16*, 255−267. (g) Kahn, O. In *Molecular Magnetism;* VCH Pulishers: New York, 1993; pp 52−85.

(11) (a) Kahn, O.; Launay, J. P. *Chemtronics* **1988**, *3*, 140. (b) Kahn, O.; Krobert, J.; Jay, C. *Adv. Mater.* **1992**, *4*, 718. (c) Launay, J. P. In *Molecular Electronic Devices II*; Carter, F. L., Ed.: Marcel Dekker: New York, 1987. (d) Joachim, C.; Launay, J. P. *J. Mol. Electron.* **1990**, *6*, 37. (e) Hush, N. S; Wong, A. T.; Bacskay, G. B.; Reimers, J. R. *J. Am. Chem. Soc.* **1990**, *112*, 4192. (f) Aviram, A. *Int. J. Quant. Chem.* **1992**, *42*, 1615. (g) *Molecular Electronics : Materials and Methods*; Lazarev, P. I., Ed.: Kluwer Academic Publishers: Dordrecht, The Netherlands, 1991. (f) *Molecular Electronics and Molecular Electronic Devices*; Sienick, K., Ed.; CRC Press: Boca Raton, FL, 1994.

(12) (a) Gutlich, P.; Hauser, A.; Spiering, H. *Angew. Chem., Int. Ed. Engl.* **1994**, *33*, 2024−2054. (b) Gutlich, P.; Hauser, A. *Coord. Chem. Rev.* **1990**, *97*, 1.

(13) (a) Jay, C.; Groliere, F.; Kahn, O.; Krober, J. *Mol. Cryst. Liq. Cryst.* **1993**, *234*, 255. (b) Krober, J.; Codjovi, E.; Kahn, O.; Groliere, F. *J. Am. Chem. Soc.* **1993**, *115*, 9810. (c) Kahn, O.; Krobert, J.; Jay, C. *Adv. Mater.* **1992**, *4*, 718.

(14) (a) Hauser, A. *Chem. Phys. Lett.* **1993**, 202, 173. (b) Hauser, A. *Coord. Chem. Rev.* **1991**, *111*, 275.

(15) Roux, C.; Adams, D. M.; Itie, J. P.; Pollian, A.; Hendrickson, D. N.; Verdaguer, M. *Inorg. Chem.* **1996**, *35*, 2846−2852.

(16) Adams, D. M.; Li, B.; Simon, J. D.; Hendrickson, D. N. *Angew. Chem., Int. Ed. Engl.* **1995**, *34*, 1481.

(17) (a) Hauser, A. *Comments Inorg. Chem.* **1995**, *17*, 17−40. (b) Hauser, A.; Vef, A.; Adler, P. J. *Chem. Phys.* **1991**, *95*, 8710.

ligand bond length changes for Fe^{II} spin crossover complexes are in the range of 0.16−0.22 Å. The cobalt valence tautomeric transformation is similarly characterized by large metal−ligand bond length changes of ca. 0.18 Å, as well as ligand bond length changes. Furthermore, since spin crossover and valence tautomerism can be thermally driven, the energy separations between the two involved states are of similar magnitude and are on the order of kT in the 150−350 K range. The rate of valence tautomerism will also be determined by the magnitude of electronic coupling between the ls-Co^{III} and hs-Co^{II} states, which is influenced by spin differences and orbital overlap. Symmetry and spin restrictions have been shown to influence the dynamics of electron transfer in linked $Ru^{II}-Co^{III}$ molecular complexes.[18] Furthermore, magnetic exchange coupling has been shown to influence the intensity of optical absorption characteristics of metal complexes by relaxing spin forbiddeness.[19]

The goals of the present research were 3-fold. First, we present detailed solution variable temperature UV-vis-near IR spectroscopic and magnetic susceptibility data for a series of complexes showing the dramatic magnetic and optical changes which accompany the valence tautomeric interconversion. Second, we discuss the thermodynamic basis of the thermally driven valence tautomeric interconversion in solution (i.e., process b). Since the valence tautomeric interconversion can be thermally induced, it is possible to obtain the equilibrium curves from which the values for the free energy change ΔG, the enthalpy difference ΔH, and the entropy gain ΔS can be extracted. Third, the microscopic details of the kinetic mechanism of process b are elucidated via variable temperature nanosecond and picosecond time-resolved optical experiments. The laser flash data for the the valence tautomeric process are analyzed in terms of the quantum mechanical theory of radiationless transitions proposed by Buhks et al.[20] to describe spin conversion processes in solution.

Experimental Section

Synthesis and Sample Preparation. All compounds were prepared according to published procedures.[1] The solution samples used for UV-vis absorption spectroscopy and laser photolysis studies were prepared in an oxygen and water free drybox under an atmosphere of Ar. Samples were sealed in 1 cm quartz cuvettes and were typically 5.0×10^{-4} M. Polymer samples were prepared by solution casting polystyrene (280 000 MW) and the complex (5% w/w) dissolved in methylene chloride onto small glass dishes. The solvent was evaporated, and the plastic films were removed from the glass.

Spectroscopic Measurements. Variable temperature electronic absorption spectra were recorded in the 320−820 nm range for solutions of the complexes on a Hewlett Packard model 8452A diode array spectrophotometer. Temperature control above room temperature was achieved utilizing a Hewlett Packard model 89054A thermostated cell holder connected to a Fisher Scientific Model 800 Isotemp circulating bath. Temperature control below room temperature was achieved using a Janis Model 8DT-SVT-OPT optical dewar. Variable temperature electronic absorption spectra for polymer samples in the 300−3000 nm range were collected on a Cary 5e spectrophotometer equipped with a closed-cycle-refrigerated cryostat in the laborartory of Prof. Hans Güdel at the University of Bern, Switzerland. Polymer samples were attached directly to the refrigerated arm of the cryostat with copper grease to insure good thermal conduction.

Magnetic Susceptibility Measurements. Direct current (dc) magnetic susceptibility measurements were carried out on a Quantum Design MPMS SQUID susceptometer equipped with a 55 kG magnetic field and operating in the 1.7−400 K temperature range. All measurements were collected in a field of 10 kG. A special quartz SQUID cell was designed for measurements performed on these dilute solutions with weak signals. The cell consists of a sample area (20 mm × 8 mm, approximate volume 0.75 mL) which is open at one end and to which is attached at each end quartz tubing (100 mm × 4 mm). The overall length of the cell is 220 mm. A machined Delrin cap with O-rings seals the cell. Solutions of all complexes were prepared in a glovebox under an atmosphere of argon by dissolving ∼0.5−1.0 mg of the complex in ∼0.7 g of toluene-d_8. All samples were dissolved in toluene-d_8 at a concentration of $\sim 1 \times 10^{-3}$ M. Measurements were collected from high temperature to low temperature. Deuterated toluene was used to ensure stable reproducible base lines.[21] Background correction data were collected from magnetic susceptibility measurements on the sealed quartz tube containing only toluene-d_8, and these data were subtracted from the magnetic susceptibility data for the complex. Diamagnetic corrections estimated from the Pascal constants were applied to all data for determination of the molar paramagnetic susceptibilities of the compounds.

Nanosecond Transient Absorption Spectroscopy. Complete details of the nanosecond time-resolved laser apparatus were given previously and will only be summarized here.[22] The nanosecond time-resolved laser photolysis apparatus center piece is a Lambda-Physik LPX 205iC rare-gas laser configured for XeCl. The laser was operated in a single-shot mode at a pressure of ∼3.3 atm with a 22.0 kV electrical discharge to produce ∼28 ns pulses at 308 nm. This pulse served as the pump source for a Lambda-Physik model Fl3002 dye laser. The dye used for all experiments was Fluorescein 27 dissolved in MeOH which allowed for tunable excitation in the range of 550−590 nm. The output pulse for the dye laser had a 24 ns full width at half maximum (FWHM) line width as measured by diffuse scattering into a Hamamatsu R1547 photomultiplier tube (PMT). This served as the pump source for the laser experiments.

The probe beam consisted of a high-energy Xe flash lamp operated at variable applied voltage of ca. −800 V dc with a pulse duration of ∼4 μs FWHM. The laser and pump beams are oriented relative to each other at a 90° angle in the front portion of a 10 mm optical cell. After passing out of the sample, the probe beam is focused onto the slit of a Instruments SA model H20 monochromator. The R1547 tube was coupled directly to the end of the monochromator at an applied voltage of −500 V dc. The output from the PMT was monitored using a Tektronix 7912AD digitizing oscilloscope, and the data were collected using a Tektronix PEP 301 controller with the TekMAP driver software. Synchronization of the probe beam, oscilloscope, and excimer laser were accomplished by a electronic timing circuit of local design. The instrument response function (IRF) of the system is 24 ns FWHM. The high degree of reproducibility of the IRF allows us to analyze our data via integral deconvolution, which extends our time resolution to below 10 ns. All data presented are a signal average of 10 transients, and the data were analyzed using computer programs of local origin.

Variable temperature measurements were performed using a Janis Model 8DT-SVT-OPT optical dewar. Temperature control was achieved with a Lakeshore Model DST-80D temperature controller and DT-47-SD-13 silicon diodes. Diodes were installed above and below the sample region, and the measured temperature was taken as the average of the two readings.

Picosecond Transient Absorption Spectroscopy. Picosecond time-resolved pump/probe optical experiments were carried out using a mode-locked Q-switched and cavity-dumped Nd-YAG laser and synchronously pumped dye laser in the laboratory of Professor John D. Simon at the University of California at San Diego. A description

(18) (a) Song, X.; Lei, Y.; Van Wallendal, S.; Perkovic, M. W.; Jackman, D. C.; Endicott, J. F.; Rillema, D. P. *J. Phys. Chem.* **1993**, *97*, 3225. (b) Endicott, J. F.; Song, X.; Watzky, M. A.; Buranda, T. *J. Photochem. Photobiol., A* **1994**, *82*, 181. (c) Watzky, M. A.; Song, X.; Endicott, J. F. *Inorg. Chim. Acta* **1994**, *226*, 109.

(19) (a) Benelli, C.; Dei, A.; Gatteschi, D.; Gudel, H.; Pardi, L. *Inorg. Chem.* **1989**, *28*, 3089. (b) Gudel, H. In *Magneto-Structural Correlations in Exchanged Coupled Systems*; Willett, R. D., Gatteschi, D., Kahn, O., Eds.; Reidel: Dordrecht, The Netherlands, 1985. (c) McCarthy, P. J.; Gudel, H. U. *Coord. Chem. Rev.* **1988**, *88*, 69.

(20) Buhks, E.; Navon, G.; Bixon, M.; Jortner, J. *J. Am. Chem. Soc.* **1980**, *102*, 2918.

(21) Day, E. P. *Methods Enzymol.* **1993**, *227*, 437−463.

(22) McCusker, J. K.; Rheingold, A.; Hendrickson, D. N. *Inorg. Chem.* **1996**, *35*, 2100.

Table 1. Transition Temperatures ($T_{1/2}$), Enthalpy Changes (ΔH), and Entropy Changes (ΔS) for the Valence Tautomeric Interconversion Evalulated from Magnetic Susceptibility Data: Activation Energies (E_a) and Preexponential Factors (A) Evaluated from Variable Temperature Rate Data for Back Valence Tautomerization[a]

complex	$T_{1/2}$ [K]	E_a [cm^{-1}]	ln A	ΔH [cm^{-1}]	ΔH [kJ mol^{-1}]	ΔS [J mol^{-1} K^{-1}]
1 phen	226.6	858	20.73	2238	26.77	118.1
2 bpy	277.0	582	20.14	3056	36.56	133.1
3 dmbpy	286.6	1088	23.36	3206	38.36	133.8
4 dpbpy	350.0	856	24.49	1717	21.33	60.6

[a] All data were determined for toluene solutions of complexes **1**−**4**.

of this apparatus is given in the literature.[23] This spectrometer has a ~90 ps FWHM pulse width with excitation at 532 nm. The probe beam operates from a dye laser and temporal resolution is achieved by an optical delay line. The apparatus is capable of delays out to ~3 ns. Data were also fit by deconvolution of the instrument response function.

Results and Discussion

Previously, it was established[1] that the σ-donating and π-backbonding abilities of the diiminium counterligand (symbolized N⁀N) can subtly modulate the energy difference between ls-Co^{III} and hs-Co^{II} tautomers. Replacement of the counterligand leads to shifts in the critical temperature $T_{1/2}$, the point where $K_{eq} = 1$ in the valence tautomeric equilibrium (eq 2):

$$\text{ls-[Co}^{III}\text{(SQ)(CAT)(N⁀N)]} \underset{k_{bvt}}{\overset{k_{fvt}}{\rightleftharpoons}} \text{hs-[Co}^{II}\text{(SQ)}_2\text{(N⁀N)]} \qquad (2)$$

In this paper, the results obtained for a series of four complexes are presented where the counterligand is systematically varied. In Table 1, the four diiminium ligands are listed.

Thermodynamic Basis of Valence Tautomerism. The idealized electronic configurations of the ls-Co^{III} and hs-Co^{II} tautomers in octahedral symmetry (O_h) are $(t_{2g})^6(e_g^*)^0(\pi^*_{CAT})^2(\pi^*_{SQ})^1$ and $(t_{2g})^5(e_g^*)^2(\pi^*_{SQ1})^1(\pi^*_{SQ2})^1$, respectively. The d-orbitals are split into the familiar t_{2g} and e_g^* set, and the ligand π^* orbitals contain a single electron in the SQ^- oxidation state and two electrons in the CAT^{2-} oxidation state. The ls-[Co^{III}(SQ)(CAT)] to hs-[Co^{II}(SQ)$_2$] interconversion is characterized by an elongation in the the metal to ligand bond distances, since the e_g^* σ-antibonding orbitals in the ls-Co^{III} form are unoccupied and doubly occupied in the hs-Co^{II} form. The interconversion of complex **1**, ls- [Co^{III}(3,5-DTBSQ)(3,5-DTBCAT)(phen)]·C_5H_6-CH_3 in the solid state to hs-[Co^{II}(3,5-DTBSQ)$_2$(phen)]·C_5H_6-CH_3, has been characterized crystallographically.[1] The average metal−ligand bond length change (Δr) has been shown to be 0.18 Å. hs-[Co^{II}(SQ)$_2$] complexes generally have average metal−ligand bond lengths that are 0.16−0.22 Å longer than those in ls-Co^{III} valence tautomers.[24] The magnitude of this change is the same as those seen in the Fe^{II} spin crossover complexes which undergo the transformation from low-spin $[(t_{2g})^6(e_g^*)^0]$ to high-spin $[(t_{2g})^4(e_g^*)^2]$. Notably though, in the cobalt valence tautomeric interconversion not only are there large metal−ligand bond length changes but also internal *o*-quinone ligand bond length changes of a lesser magnitude, since the valence tautomerism is an electron transfer process.

The electronic lability associated with the valence tautomeric interconversion can be illustrated with the aid of the one-dimensional potential energy diagram shown in Figure 1. The complex can exist in one of two states that are represented by the two harmonic potential energy curves shown in Figure 1. The potential energy of the complex is plotted as a function of the reaction coordinate. The nuclear configurations of the ls-Co^{III} and hs-Co^{II} valence tautomers differ mainly in the metal−ligand bond distances. It is reasonable to assume to a first approximation that the reaction coordinate for valence tautomerism will be approximately equivalent to the totally symmetric metal−ligand breathing normal coordinate. The energy of the symmetric metal ligand stretching vibration in ls-Co^{III} complexes is ~450 and ~350 cm^{-1} for hs-Co^{II} complexes.[25] The wells are shifted relative to each other by a value reflecting the ~0.18 Å metal−ligand bond length change. Furthermore, the energy separation between the two lowest levels, $\Delta E \approx \Delta H = H_{hs-Co^{II}} - H_{ls-Co^{III}}$, is positive where the hs-Co^{II} state lies higher in energy. The energy separation in the four cobalt complexes studied is on the order of kT at room temperature.

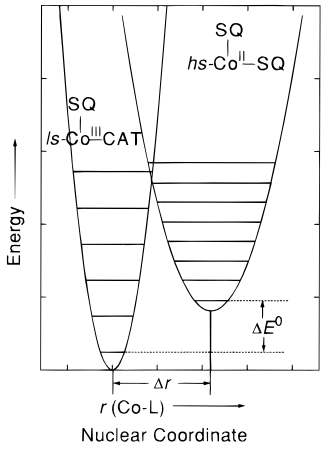

Figure 1. Schematic representation of the potential energy surface describing the ls-[Co^{III}(SQ)(CAT)(N⁀N)] to hs-[Co^{II}(SQ)$_2$(N⁀N)] valence tautomeric interconversion. The energy difference $\Delta E°$ is on the order of 6 kT for thermally driven valence tautomerism. The nuclear coordinate to a first approximation is the symmetric metal−ligand stretching mode.

In analogy to the extensively studied *low-spin* to *high-spin* crossover phenomenon observed in iron complexes,[10] the interconversion between valence tautomers is an entropy driven process. The valence tautomerism is characterized by a large entropy gain where

$$\Delta S = \Delta S_{hs-Co^{II}} - \Delta S_{ls-Co^{III}} = \Delta S_{elec} + \Delta S_{vib} > 0 \qquad (3)$$

The valence tautomeric interconversion from ls-Co^{III} to hs-Co^{II} leads to a gain in electronic entropy (ΔS_{elec}) due to the higher spin state degeneracy of the hs-Co^{II} form. At low temperatures, the ls-Co^{III} tautomer has an $S = {}^1/_2$ ground state (ls-Co^{III} d^6 $S = 0$; CAT^{2-} $S = 0$; SQ^- $S = {}^1/_2$ radical); whereas at higher temperatures, the exchange coupled hs-Co^{II} tautomer (hs-Co^{II} $S = {}^3/_2$, and two $S = {}^1/_2$ SQ^- radicals) has one $S = {}^5/_2$, one $S = {}^1/_2$, and two $S = {}^3/_2$ states thermally populated due to very weak magnetic exchange interactions.[26] Furthermore, the longer metal−ligand bond lengths of the hs-Co^{II} tautomer result in lower energy vibrations and a higher density of vibrational states in hs-Co^{II} form than in the ls-Co^{III} form. Thus, the thermal population of tautomeric states is dictated by the Gibbs free

(23) Xie, X.; Simon, J. D. *Opt. Commun*. **1989**, *69*, 303.
(24) (a) Pierpont, C. G.; Buchanan, R. M. *Coord. Chem. Rev*. **1981**, *38*, 45. (b) Pierpont, C. G.; Lange, C. W. *Prog. Inorg. Chem*. **1994**, *41*, 331.
(25) Buhks, E.; Bixon, M.; Jortner, J. *J. Phys. Chem*. **1981**, *85*, 3763.
(26) (a) Lynch, M. W.; Buchanan, R. M.; Pierpont, C. G.; Hendrickson, D. N. *Inorg. Chem*. **1981**, *20*, 1038. (b) Lange, C. W.; Conklin, B. J.; Pierpont, C. G. *Inorg. Chem*. **1994**, *33*, 1276.

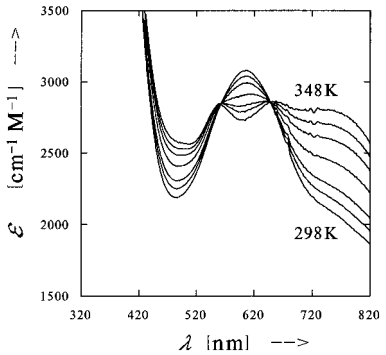

Figure 2. Temperature dependence of the electronic absorption spectrum of a toluene solution of [Co(3,5-DTBSQ)(3,5-DTBCAT)-(dpbpy)] (**4**) obtained at 298, 303, 308, 318, 328, and 348 K. The molar extinction coefficient ϵ is plotted versus the wavelength λ.

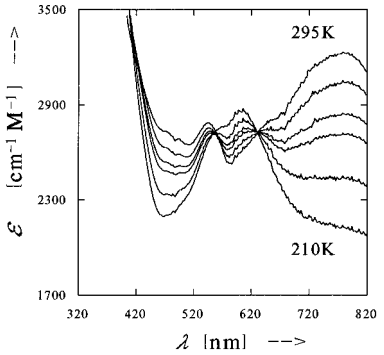

Figure 3. Temperature dependence of the electronic absorption spectrum of a toluene solution of [Co(3,5-DTBSQ)$_2$(phen)] (**1**) obtained at 295, 260, 240, 230, 220, and 210 K. The molar extinction coefficient ϵ is plotted versus the wavelength λ.

energy difference where

$$\Delta G = \Delta G_{\text{hs}-\text{Co}^{\text{II}}} - \Delta G_{\text{ls}-\text{Co}^{\text{III}}} = \Delta H - T\Delta S \qquad (4)$$

The hs-Co^{II} tautomer zero-point energy must lie at higher enthalpic energy than that for the ls-Co^{III} form. At low temperatures, $T\Delta S$ is negligible compared to ΔH, and consequently if $\Delta H > kT$ only the Co^{III} state is populated. However, $T\Delta S$ is not negligible at higher temperatures, and ΔG will change sign at a critical temperature $T_{1/2}$ where $\Delta G = 0$ and $\Delta H = T\Delta S$. At higher temperatures, the Co^{II} tautomeric state may be almost completely populated if ΔS is large enough. Decreasing the energy (i.e., enthalpy) separation between tautomeric forms will ultimately lead to a decrease in the values of $T_{1/2}$. This explains the trend seen for complexes **1**, **2**, and **3**, however other factors must come into play for complex **4**.

Variable Temperature Optical Spectroscopy. Variable temperature electronic absorption spectra (320−820 nm) were run for all complexes. In toluene solution, all four of the complexes show temperature-dependent spectra that indicate the presence of the valence tautomeric equilibrium as given in eq 2. The temperature dependence of the spectrum for [Co(3,5-DTBSQ)(3,5-DTBCAT)(dpbpy)] (**4**) in toluene is shown in Figure 2. At room temperature, there is a band at 600 nm with a shoulder at ∼800 nm which is characteristic of the ls-Co^{III} tautomeric form of the complex. As the temperature of the toluene solution is increased from 298 to 348 K, the intensity of the 600 nm band decreases while a band at ∼770 nm increases in intensity. This 770 nm band is characteristic of the hs-Co^{II} form of the complex, which also shows bands at ∼655 and ∼545 nm. As can be seen, the molar extinction coefficients of the bands are ∼2500 M^{-1} cm^{-1}, indicating that they are likely of the charge-transfer-type. The exact origin of the ls-Co^{III} charge transfer transition at ∼600 nm is unknown but it probably originates from transitions from filled molecular π-orbitals to the unoccupied SQ π*-orbital. This band may also contain some contribution from a ligand to metal charge transfer (LMCT) transition involving the CAT^{2-} ligand and the cobalt ion. The band at 770 nm is likely a metal to ligand charge transfer (MLCT) transition of the hs-Co^{II} tautomer. The band at 548 nm is associated with the Co^{II} tautomer and is likely a ligand field (LF) type transition. The presence of isosbestic points is strong evidence that only two different species are present in solution and that the valence tautomeric equilibrium in eq 2 is present.[27]

(27) Harris, D. C.; Bertolucci, M. D. In *Symmetry and Spectroscopy: An Introduction to Vibrational and Electronic Spectroscopy*; Dover Publications: New York, 1989; pp 416−418.

The temperature dependence of the electronic absorption spectrum of a toluene solution of the dmbpy complex **3** is similar to that seen for the dpbpy complex (figure available in Supporting Information). At 298 K, the spectrum for **3** in solution shows contributions from both the ls-Co^{III} and hs-Co^{II} tautomers, having the characteristic 600 nm transition of the ls-Co^{III} and the 770 and 545 nm transitions of the hs-Co^{II} tautomer. As the temperature is increased from room temperature to 348 K, the 600 nm absorption band decreases significantly and the 545 and 770 nm bands become more intense. Above 348 K, the absorption spectrum does not change significantly. Thus, it is evident that the $T_{1/2}$ value for complex **3** is lower than that for complex **4** and is somewhere close to room temperature.

In contrast, the bpy complex **2** and phen complex **1** in toluene solution at 298 K display the spectral characteristics of the hs-Co^{II} tautomer. The absorption spectra of complexes **1** and **2** in toluene show only a small increase in the 770 nm band of the hs-Co^{II} tautomer upon increasing the temperature from 298 to 328 K. Figure 3 shows the temperature dependence of the electronic absorption spectrum of a toluene solution of phen complex **1**. At 295 K, this spectrum is highly characteristic of a Co^{II} tautomer, as indicated by an intense broad band at 780 nm with a shoulder at ∼660 nm and a weaker band at 548 nm. When the temperature is decreased from 295 to 210 K, the intensity of the 780 nm band decreases appreciably, while a band at ∼600 nm characteristic of the Co^{III} tautomer appears. At 210 K, the phen complex has almost completely converted to the ls-Co^{III} form.

Large changes in the optical spectrum also occur in the near infrared (near IR) region of spectrum. Figure 4 shows the temperature dependence of the electronic absorption spectrum of complex **1** doped into a polystyrene (280 000 MW) polymer film monitored from 300 to 3000 nm in the temperature range of 15−295 K. The changes in the visible region of the spectrum are similar to those found for the toluene solution of complex **1**. At 15K, the absorptions arise solely from the ls-[Co^{III}(SQ)-(CAT)(phen)] valence tautomer. The 600 nm band displays a progression of shoulders at ∼560, ∼800, and ∼1000 nm. At low temperatures, a band appears at 2500 nm with a shoulder at 1670 nm, which is only associated with the ls-Co^{III} tautomer. In comparison to the solution spectra, an approximate molar extinction coefficient (ϵ) at the maximum absorption of the 2500 nm band of ∼2200 cm^{-1} M^{-1} can be estimated. Density functional LCAO calculations indicate that this band is the mixed valence intervalence charge transfer (IT) band involving excitation of an electron from the CAT^{2-} to the SQ^{-} ligand.[28]

The environment about the valence tautomeric complex can influence the $T_{1/2}$ for the interconversion, presumably by

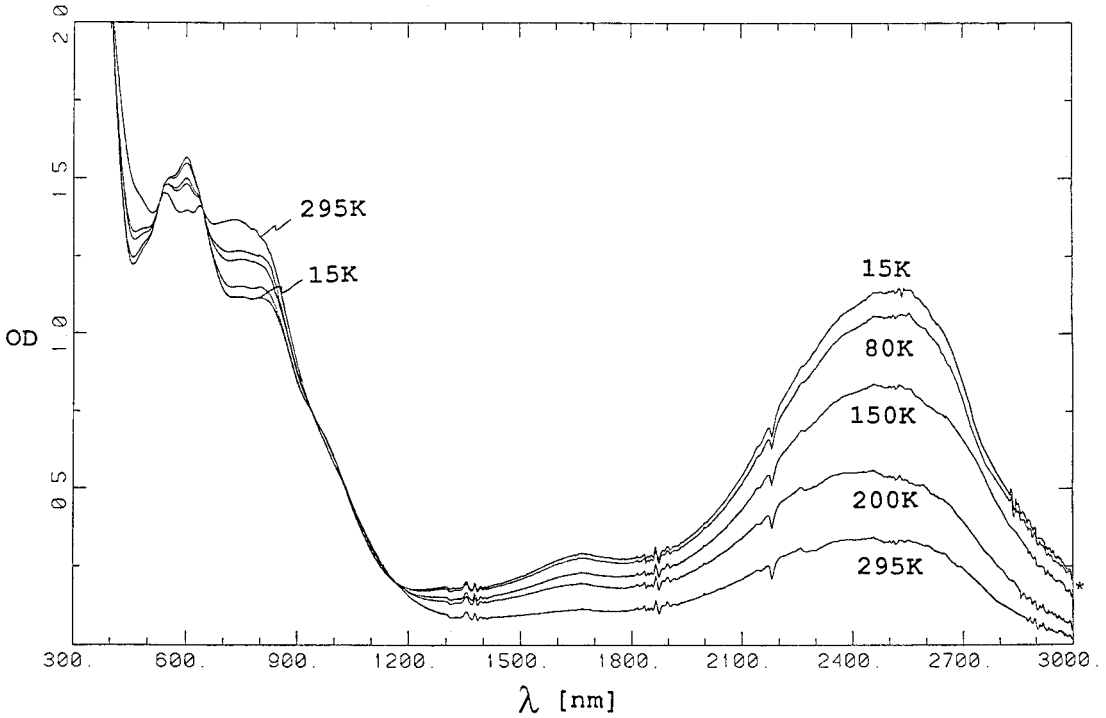

Figure 4. Temperature dependence of the electronic absorption spectrum of a polystyrene film of [Co(3,5-DTBSQ)$_2$(phen)] (**1**) obtained at 295, 200, 150, 80, and 15 K. The optical density (OD) is plotted versus the wavelength λ.

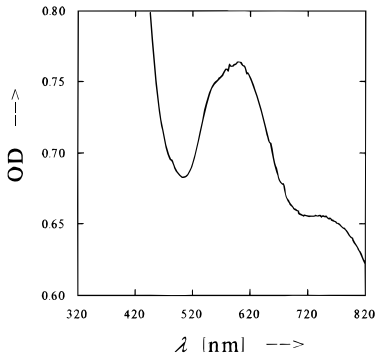

Figure 5. Electronic absorption spectrum of a polystyrene film (5% w/w) of [Co(3,5-DTBSQ)(3,5-DTBCAT)(bpy)] (**2**) at 298 K. The optical density (OD) is plotted versus the wavelength λ.

modulating the energy separation between the tautomeric forms. Figure 5 displays the electronic absorption spectrum of complex **2** doped into a polystyrene matrix at 298 K. The complex displays the absorption characteristics of the ls-[Co^{III}(CAT)-(SQ)(bpy)] tautomer; whereas, at room temperature in toluene solution, the complex shows the characteristics of the hs-Co^{II} tautomer. Similarly, the room temperature electronic absorption spectrum of dmpby complex **3** doped into a polystyrene film shows that the system is in the ls-Co^{III} tautomeric state. This contrasts with the 298 K toluene solution which shows that an appreciable amount of the Co^{II} form is present. Likewise the absorption spectrum of phen complex **1** doped into a polystyrene matrix (Figure 4) shows that an appreciable amount of both tautomeric forms are present at 298 K, while the 298 K toluene solution spectrum shows only the characteristics of the hs-Co^{II} form. Relative to a toluene solution, the polymer matrix increases the energy separation between valence tautomeric forms. This likely arises from the more compact polymeric glass structure which serves to favor the much smaller ls-Co^{III} tautomer. Previous work has shown that the solvent dielectric can also shift $T_{1/2}$.[4a,16] It is evident that these valence tautomeric complexes are quite sensitive to their environment.

The ls-[Co^{III}(SQ)CAT)(N⁀N)] valence tautomer is nearly a symmetric mixed valence complex. Intramolecular electron transfer interconverts the CAT^{2-} and SQ^{-} ligands. From the characteristics of the IT transition absorption it is possible to calculate the degree of electronic coupling and barrier height to interconversion from the well-known Hush formula[29] for mixed valence complexes given in eq 5.

$$H_{ab} = (2.05 \times 10^{-2})[\epsilon_{max}\Delta\nu_{1/2}/\nu_{max}]^{1/2}\nu_{max}/r \qquad (5)$$

In this equation, ϵ_{max} is the maximum extinction coefficient of the absorption band in M^{-1} cm^{-1}, $\Delta\nu_{1/2}$ is the band width at half ϵ_{max}, ν_{max} is the energy of the absorption in cm^{-1}, and r is the distance between donor and acceptor wave functions. Using the values of r = 2.83 Å (shortest distance between oxygen atoms), ϵ_{max} = 2200 M^{-1} cm^{-1}, $\Delta\nu_{1/2}$ = 1200 cm^{-1}, and ν_{max} = 4000 cm^{-1}, H_{ab} is calculated to be 752 cm^{-1} with the barrier height as 248 cm^{-1}. Since the barrier to interconversion is estimated to be 248 cm^{-1}, it is likely that at room temperature the complex is thermally interconverting between the two mixed valence forms.

Variable Temperature Magnetic Susceptibility. Large changes in the magnetic susceptibilities also accompany the valence tautomeric interconversion. Variable temperature solution magnetic susceptibility data were collected for complexes **1**−**4** in toluene solution at ∼1.0 × 10^{-3} M. Values of $\chi_M T$, where χ_M is the measured molar paramagnetic susceptibility, range from the low-temperature limit of 0.37−0.54 cm^3 K mol^{-1} to 2.35 cm^3 K mol^{-1} (μ_{eff} = 4.34 μ_B) in the high temperature limit. Previous solution magnetic measurements of complex **2** also gave a $\chi_M T$ value of 2.35 cm^3 K mol^{-1} in the high-temperature limit.[30] At low temperatures the $\chi_M T$ values are close to the value expected for a single unpaired electron on the semiquinonate ligand of the ls-[Co^{III}(SQ)(CAT)(N⁀N)] tautomer. If there were no intramolecular magnetic exchange

(28) Adams, D. M.; Noodleman, L.; Hendrickson, D. N. Submitted for publication.

(29) Hush, N. S. *Prog. Inorg. Chem.* **1967**, 8, 357.

interactions present in hs-[$Co^{II}(SQ)_2(N\frown N)$] and if the hs-Co^{II} ion exhibited a spin-only ($g = 2$) magnetism, then the value of $\chi_M T$ should be 2.62 cm^3 K mol^{-1} ($\mu_{eff} = 4.58\ \mu_B$). Usually a hs-Co^{II} ion has considerable orbital angular momentum with μ_{eff} in the range of 4.8−5.0 μ_B, which corresponds to $\chi_M T$ in the range of 2.9−3.1 cm^3 K mol^{-1}. It is not clear why the high-temperature limiting value of the experimental $\chi_M T$ value is so much lower; however, it is found for many such Co^{II} valence tautomeric complexes in solution. Furthermore, similar relatively low values of $\chi_M T$ at the higher temperatures were found even for solid samples. For example, [Co(3,5-DTBSQ)$_2$-(phen)], recrystallized from methylcyclohexane to give a non-solvated complex, shows $\mu_{eff} = 4.1\ \mu_B$ at 300 K. In fact, this nonsolvated phen complex persists as a hs-Co^{II} complex throughout the 2−320 K region, whereas the toluene solvate of the same complex converts abruptly in the 200−260 K region between the hs-Co^{II} and ls-Co^{III} tautomeric forms. One possible origin for lower values of $\chi_M T$ for a hs-[$Co^{II}(SQ)_2(N\frown N)$] complex is the presence of intramolecular magnetic exchange interactions between SQ^- ligands and the Co^{II} ion.

In order to evaluate thermodynamic parameters such as ΔH and ΔS from solution magnetic susceptibility data, we have assumed a two state equilibrium between the ls-Co^{III} and hs-Co^{II} tautomers as in eq 2. The thermodynamic parameters for the dynamic equilibrium were obtained using the following equations:

$$f_{hs-Co^{II}} = (\chi_{obs}T - \chi_{ls-Co^{III}}T)/(\chi_{hs-Co^{II}}T - \chi_{ls-Co^{III}}T) \quad (6)$$

$$K_{eq} = (f_{hs-Co^{II}})/(f_{ls-Co^{III}}) = (f_{hs-Co^{II}})/(1 - f_{hs-Co^{II}}) \quad (7)$$

$$\Delta G = -RT\ln(K_{eq}) \quad (8)$$

In these equations, χ_{obs} is the molar susceptibility at a given temperature and $\chi_{hs-Co^{II}}$ and $\chi_{ls-Co^{III}}$ are the molar susceptibilities of the pure hs-Co^{II} and ls-Co^{III} components, respectively, and $f_{hs-Co^{II}}$ and $f_{ls-Co^{III}}$ are the corresponding mole fractions. The value of $\chi_{hs-Co^{II}}T$ for a hs-Co^{II} complex was taken as 2.35 cm^3 K mol^{-1} from the high-temperature plateau value for phen complex **1** in solution. In fitting the susceptibility data for these complexes, it was assumed that there was no temperature dependence of $\chi_M T$ for the hs-Co^{II} tautomer. The value of $\chi_{ls-Co^{III}}T$ was evaluated separately for each system from the low temperature data. Using eqs 4, 6, and 8 results in eq 9 which gives $f_{hs-Co^{II}}$ as a function of T, ΔH and ΔS.

$$f_{hs-Co^{II}} = 1/[\exp(\Delta H/RT - \Delta S/R) + 1] \quad (9)$$

Figure 6 shows the solution magnetic susceptibility data plotted to display $f_{hs-Co^{II}}$ as a function of temperature. The solid lines represents the best fits of the data to eq 9, and Table 1 lists the values obtained for ΔH and ΔS from the fitting for all four complexes in toluene solution. It can be seen that the data are well represented by the fit. The observed values of $T_{1/2}$ for complexes **1**−**3** correlate well with the ΔH values. The ΔH values for complexes **1**−**3** are found to be 2238, 3056, and 3206 cm^{-1}, respectively. This confirms the prediction that the counter ligand can subtly modulate the energy separations. The entropy gains ΔS for these three complexes range from 118.1 to 133.1 J mol^{-1} K^{-1} and are somewhat higher than those observed in Fe^{II} spin crossover complexes. Thermodynamic data were previously reported[30] for complex **2** and agree with the values reported here. Complex **4** presents a more gradual transition, and consequently ΔH and ΔS are found to be 1717 cm^{-1} and 60.6 J mol^{-1} K^{-1}, respectively. The complete equilibrium curve

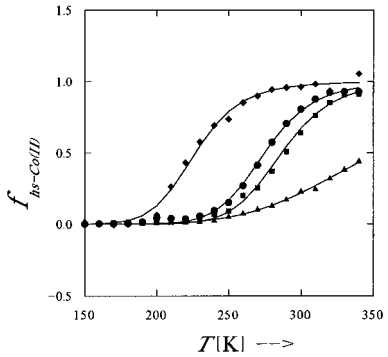

Figure 6. Plot of the fraction high-spin Co^{II} valence tautomeric state versus temperature evaluated from solution magnetic susceptibility data for: (◆) [Co(3,5-DTBSQ)$_2$(phen)] (**1**); (●) [Co(3,5-DTBSQ)$_2$(bpy)] (**2**); (■) [Co(3,5-DTBSQ)$_2$(dmbpy)] (**3**); and (△) [Co(3,5-DTBSQ)$_2$(dpbpy)] (**4**). The solid lines represent fits of the data to eq 10.

for **4** could not be obtained since $T_{1/2}$ is 350 K and magnetic measurements could not be performed above this temperature. Heat capacity measurements for the spin crossover transition in Fe^{II} complexes have given ΔS values ranging from 50 to 80 J mol^{-1} K^{-1}.[31] The electronic and vibrational entropy gain associated with the valence tautomeric interconversion are expected to be similar to those found for the Fe^{II} spin crossover phenomenon. The electronic entropy gain is given by $\Delta S_{elec} = R\ln(W_{hs-Co^{II}}/W_{ls-Co^{III}})$, where R is the gas constant and $W_{hs-Co^{II}}$ and $W_{ls-Co^{III}}$ are the electronic degeneracies of the hs-Co^{II} and ls-Co^{III} tautomers. Thus, for these valence tautomeric complexes $\Delta S_{elec} = R\ln(16/4) = 11.53$ J mol^{-1} K^{-1}. Fe^{II} spin crossover complexes display ΔS_{vib} values in the range of 50−65 J mol^{-1} K^{-1}. The cobalt valence tautomeric complexes should display values for ΔS_{vib} of similar or larger magnitude. Thus, we estimate that ΔS should be on the order of 75 J mol^{-1} K^{-1} or greater. The higher observed values of ΔS for complexes **1**−**3** could be associated with a larger vibrational entropy gain, since the interconversion is an electron transfer process and not only involves metal−ligand bond length changes as in Fe^{II} spin crossover complexes but also changes in the bond lengths and vibrational frequencies associated with the SQ^- and CAT^{2-} ligands.

Electronic Structures and Counterligand Influence. There are several ways to address the question of how does the diiminium counterligand influence the properties of a given valence tautomeric cobalt complex. On the one hand it is possible to discuss the relative σ-donation and π-backbonding of each diiminium ligand. A careful look at the highest occupied and lowest unoccupied molecular orbitals of a complex could also shed light on why certain complexes are ls-Co^{III} tautomers at room temperature, whereas others are hs-Co^{II} tautomers. In the solid state at room temperature, the dpbpy, dmbpy, and bpy complexes are ls-Co^{III} tautomers, whereas the phen complex is a hs-Co^{II} tautomer.

Figure 7 shows the frontier molecular orbitals for the $S = {}^1/_2$ ls-[$Co^{III}(SQ)(CAT)(N\frown N)$] and antiferromagnetic $S = {}^1/_2$ hs-[$Co^{II}(SQ)_2(N\frown N)$] states obtained from spin-unrestricted density functional LCAO electronic structure calculations.[28] In spin-polarized density functional theory the spin up (α) and spin down (β) electrons are treated separately, which is critical for any system with unpaired spin density.[32] Figure 7 graphically

(30) Pierpont, C. G.; Jung, O. S. *Inorg. Chem.* **1995**, *34*, 4281.

(31) (a) Sorai, M.; Seki, S. *J. Phys. Soc. Jpn.* **1972**, *33*, 575. (b) Sorai, M.; Seki, S. *J. Phys. Chem. Solids* **1974**, *35*, 555. (c) Kaji, K.; Sorai, M. *Thermochim. Acta* **1985**, *88*, 185. (d) Sorai, M.; Maeda, Y.; Oshio, H. *J. Phys. Chem. Solids* **1990**, *51*, 941.

(32) Noodleman, L.; Peng, C. Y.; Case, D.; Mouesca, J. M. *Coord. Chem. Rev.* **1995**, *144*, 199.

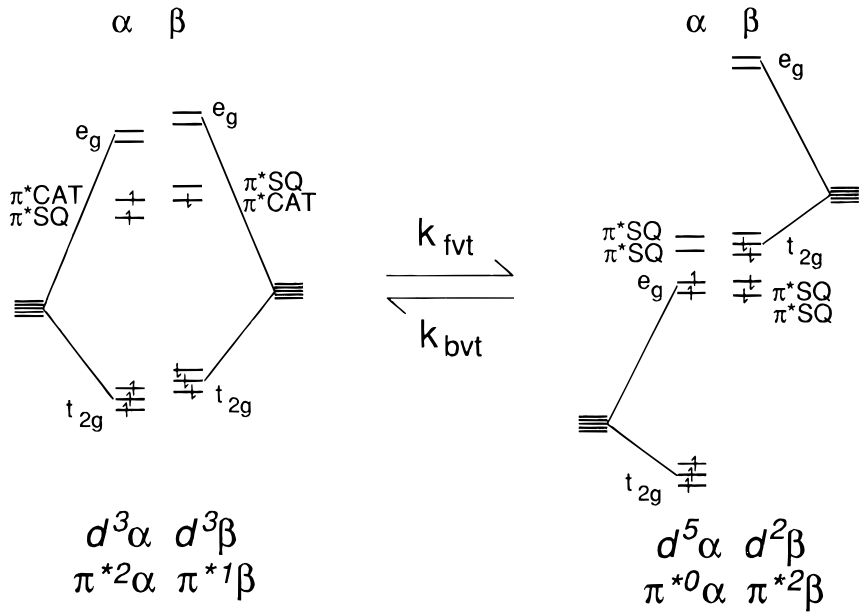

Figure 7. Idealized spin-polarized energy level diagrams of the $S = {}^1/_2$ ls-Co^{III} (left) and $S = {}^1/_2$ antiferromagnetically coupled hs-Co^{II} (right) states showing the relative ordering of α-spin and β-spin energy levels of the ligand field set (O_h symmetry notation) and π*-orbitals of the *o*-quinone-derived ligands. The $\Delta S = {}^1/_2$ spin allowed valence tautomeric interconversion likely occurs between these two states. Energy level orderings have been extracted from density function LCAO calculations (ref 28).

illustrates the idealized energy level diagrams of the spin-polarized ligand field splitting of the cobalt d-orbitals and π*-energy levels of the two quinones. The vertical axis gives the orbital energies, and the horizontal axis separates levels according to their spin index, α or β. Symmetry labels are taken from idealized O_h symmetry, where the familiar d-orbital splittings into t_{2g} and e_g* orbitals are shown. The ls-[Co^{III}-(CAT)(SQ)] valence tautomeric state has the occupation scheme: Co^{III} $d^3\alpha$ $d^3\beta$ ($S = 0$); CAT $\pi^{*1}\alpha$ $\pi^{*1}\beta$ ($S = 0$); SQ $\pi^{*1}\alpha$ $\pi^{*0}\beta$ ($S = {}^1/_2$). The quinone π*-orbitals are the highest occupied and lie relatively close in energy to the unnoccupied e_g* orbitals of the cobalt. In contrast, the $S = {}^1/_2$ antiferromagnetically coupled hs-[$Co^{II}(SQ)_2$] valence tautomeric state has the occupation scheme: Co^{II} $d^5\alpha$ $d^2\beta$ ($S = 3/2$); SQ $\pi^{*0}\alpha$ $\pi^{*1}\beta$ ($S = {}^1/_2$); SQ $\pi^{*0}\alpha$ $\pi^{*1}\beta$ ($S = {}^1/_2$). Here there is large spin polarization splitting between majority α-spin and minority β-spin 3d-energy levels, since the amount of unpaired spin has increased. Also, the ligand field splitting has been substantially reduced since the metal−ligand bond distances have increased by 0.18 Å. The spin polarization splitting for the hs-Co^{II} state slightly exceeds the ligand field splitting, and consequently, the competition favors the *high-spin* metal site.

The σ-donating and π-accepting properties of the counterligand affect the ligand field splitting of the cobalt center which ultimately leads to modulation of the energy separations between valence tautomeric states. Greater σ-donation stabilizes the ls-Co^{III} state by decreasing the total bonding energy of the complex and ensuring that the e_g* orbitals are removed in energy from the *o*-quinone π*-orbitals. Decreasing the energy of the e_g* orbitals can ultimately lead to a situation in which the e_g* orbitals lie lower in energy than the π*-orbitals which can lead to electron transfer from the ligand to the metal. Conversely, weaker σ-donation ultimately leads to the stabilization of the hs-Co^{II} state. If the ligand field splitting is smaller than the spin polarization splitting, the hs-Co^{II} state is favored. In the hs-Co^{II} tautomer greater σ-donation tends to place the occupied e_g* in α in closer energy proximity to the unoccupied π*-orbitals. If the ligand field splitting is large, then the e_g* orbitals may lie higher in energy than the π*-orbitals resulting in electron transfer from the Co^{II} center to the SQ^- π*-orbital.

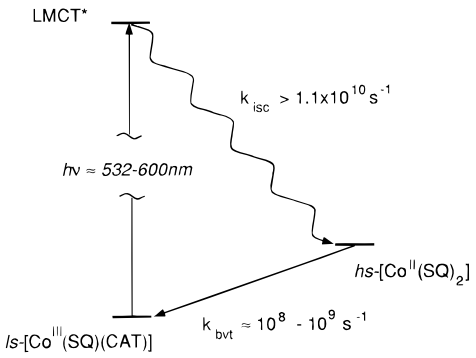

Figure 8. Jablonski diagram for the photoinduced valence tautomeric process. The laser pulse into the 600 nm charge transfer absorption band of the ls-Co^{III} tautomer results in population of a LMCT excited state. Rapid intersystem crossing produces the hs-Co^{II} state followed by a slower back valence tautomerization.

Kinetics of the Valence Tautomeric Interconversion: Laser Photolysis Studies. The strategy for pulsed laser photolysis experiments for photoinduced valence tautomerism is shown in Figure 8. The laser pulse into the 600 nm band of the ls-Co^{III} tautomer excites the complex into a LMCT excited state. Following excitation some fraction of molecules will intersystem cross from this excited state to populate the hs-Co^{II} tautomeric state. If the rates of intersystem crossing are much faster than the relaxation from the hs-Co^{II} to the ls-Co^{III} state, then it is straightforward to obtain the rate of back valence tautomerization. The change of the electronic absorption spectrum is monitored at some wavelength before, during, and after the laser pulse. Valence tautomeric complexes, like spin crossover complexes, are particularly well suited for photophysical investigations, since the electronic absorption spectra of the ground and excited states can be obtained by varying the temperature. The cobalt valence tautomeric complexes display isosbestic points in the optical spectra. Pulsed laser experiments can be employed to look for transient bleaches and absorptions around isosbestic points. The largest change in absorption between the ls-Co^{III} and hs-Co^{II} tautomers occurs in the 700−800 nm range, and in the near IR at 2500 nm. The relaxation can be best monitored at ∼770 nm as a transient absorption

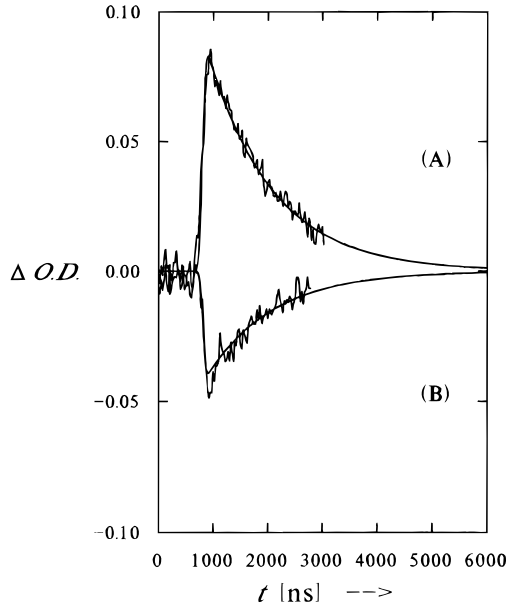

Figure 9. (A) Changes in the transient absorption (ΔOD = change in absorption) of dpbpy complex **4** in toluene at 298 K monitored at 720 nm after excitation at 532 nm. (B) Transient bleach monitored at 600 nm after excitation at 532 nm. The solid lines represent a convolution of the instrument response function with a single exponential decay, where $\tau_{obs} = 1.2$ ns for both data sets.

but also can be monitored as a transient bleach of the 600 nm transition. Detection of the optical changes in the near IR is desirable, but this is a much more difficult experiment. Currently our laser systems are not configured to monitor at these wavelengths.

Figure 9 shows the picosecond time-resolved transient curves obtained for a solution of dpbpy complex **4** in toluene (1.63×10^{-3} M) at 298 K. A 532 nm pump pulse (90 ps pulse width FWHM) into the 600 nm LMCT band of the ls-Co^{III} tautomer results in a transient absorption monitored at 720 nm and a transient bleach monitored at 600 nm. The solid line represents a convolution of the instrument response function with a single exponential decay of the form

$$\text{Change of Absorbance } (t) = \Delta[\text{OD}(t)] = A \exp(t/\tau_{obs}) \quad (10)$$

where A is a premultiplier, t is time, and τ_{obs} is the lifetime of the decay. Both of the transients are well described by single exponential functions with the same time constant of $\tau_{obs} = 1.2$ ns. Since the integral deconvolution procedure takes into account the entire pulse profile, it can be seen in Figure 9 that both the rise and decay of the signal are fit in determining the value of the observed lifetime. Since we see no indication of a rise time, the hs-Co^{II} state is formed within the experimental resolution of 90 ps. The observation of a bleach and absorption with identical kinetics around an isosbestic point indicates that we are looking at light-induced population of the hs-[$Co^{II}(SQ)_2$-(N⌒N)] state, followed by relaxation back to equilibrium. It should be noted that valence tautomers are in thermal equilibrium in solution according to eq 2. The photoinduced valence tautomerization involves a reversible first-order reaction, where

$$\tau_{obs} = 1/k_{obs} = 1/k_{fvt} + 1/k_{bvt} \quad (11)$$

and since $K_{eq} = k_{fvt}/k_{bvt}$, eq 12 results:

$$\tau_{bvt} = 1/k_{bvt} = \tau_{obs}[K_{eq} + 1] \quad (12)$$

At 298 K in toluene solution, the K_{eq} value for the dpbpy complex **4** was measured to be 0.24, and with $\tau_{obs} = 1.2$ ns, we consequently calculate $\tau_{bvt} = 1.49$ ns. The observed lifetime of the excited state of the dmbpy complex **3** in toluene (1.10×10^{-3} M) at 298 K following photoexcitation ($\lambda_{pump} = 532$ nm, $\lambda_{probe} = 720$ nm) was determined to be $\tau_{obs} = 7$ ns. The value of K_{eq} at 298 K for complex **3** is 1.35, and consequently, we find $\tau_{bvt} = 16.45$ ns. Since complexes **1** and **2** are in the hs-Co^{II} tautomeric form at room temperature in toluene solution, picosecond time-resolved spectroscopy was not attempted for these two complexes.

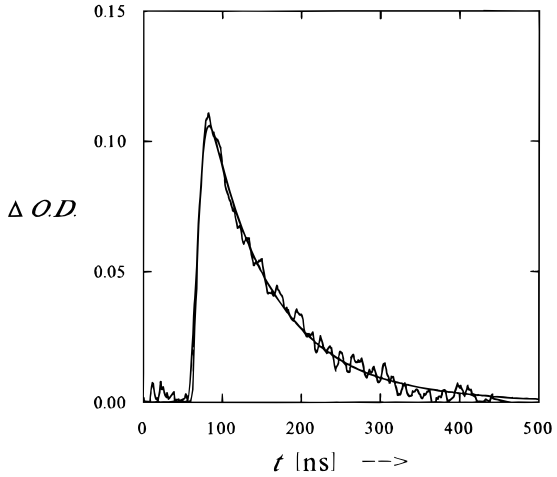

Figure 10. Transient absorption decay for bpy complex **2** monitored at 740 nm following excitation at 560 nm. Data were collected at 210 K for a toluene solution. The smooth line represents a convolution of the instrument response function with a single exponential decay where $\tau_{obs} = 102$ ns.

Variable temperature nanosecond transient absorption spectroscopy has been performed on the series of four cobalt valence tautomeric complexes. At low temperatures, all four complexes exist in the ls-Co^{III} state and the nanosecond timescale is appropriate for these compounds. The relaxation times were found to follow single exponential kinetics and were independent of monitoring wavelengths and of solution concentrations ranging from 1×10^{-4} to 5×10^{-3} M. Furthermore, there was no observed sample degradation during laser experiments for any of the molecules studied. Figure 10 shows a typical kinetic trace of the relaxation of a 5×10^{-4} M toluene solution of ls-[Co^{III}(3,5-DTBSQ)(3,5-DTBCAT)(bpy)] (**2**) at 220.5 K, following laser excitation with $\lambda_{pump} = 560$ nm and monitored at a wavelength of $\lambda_{probe} = 740$ nm. The solid line represents a convolution of the instrument response function (IRF) and a single exponential decay with $\tau_{obs} = 102$ ns. Figure 11 shows the kinetic trace of a 5×10^{-4} M toluene solution of complex **1** at 209.9 K at the same pump and probe wavelengths. Fitting of the data gives $\tau_{obs} = 262$ ns. The largest optical changes can be monitored as transient absorptions at wavelengths between 700−800 nm, since the hs-$Co^{II}(SQ)_2$ complex absorbs most strongly at these wavelengths. However transient bleaches can also be monitored. Figure 12 displays typical single-wavelength kinetic traces of the relaxation of complex **3** in a 5.0×10^{-4} M toluene solution at 200.8 K, following photoexcitation with $\lambda_{pump} = 560$ nm. The transient absorption (A) was monitored at 740 nm, and the transient bleach (B) was monitored at 570 nm. The solid lines represent a convolution of the instrument response function and a single exponential decay. Fitting of the data gives $\tau_{obs} = 187$ ns for both the transient bleach and the absorption.

The observation of isosbestic points at 545 and 560 nm in the variable temperature absorption spectrum of complex **3** shown in Supporting Information provides strong evidence that

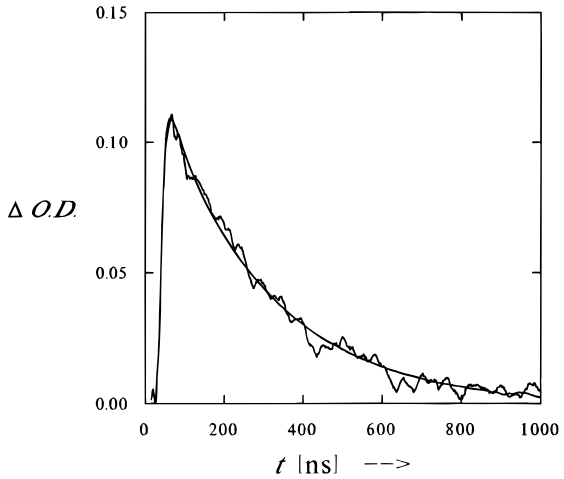

Figure 11. Transient absorption decay for phen complex **1** in toluene monitored at 740 nm following excitation at 560 nm. Data were collected at 209.9 K. The smooth line represents a convolution of the instrument response function with a single exponential decay where $\tau_{obs} = 262$ ns.

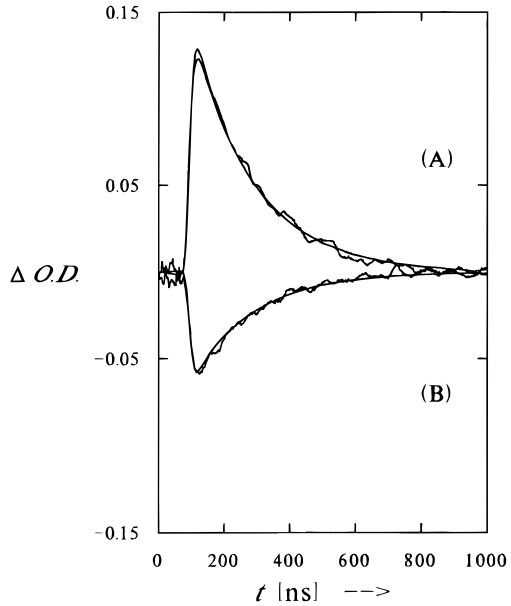

Figure 12. (A) Changes in the transient absorption (ΔOD = change in absorption) of dmbpy complex **3** in toluene at 200.8 K monitored at 740 nm after excitation at 560 nm. (B) Transient bleach monitored at 570 nm after excitation at 560 nm. The solid lines represent a convolution of the instrument response function with a single exponential decay, where $\tau_{obs} = 187$ ns for both data sets.

only two species are in solution and that the equilibrium in eq 2 is present. If the same isosbestic points occur in the transient spectrum, it may be argued that the same two states, and only those two states, are involved in the photoinitiated process. The observation again on the nanosecond timescale of identical kinetics for the bleach and absorption around an isosbestic point confirms that we are seeing population of the hs-[$Co^{II}(SQ)_2$-(N⌒N)] state. It was possible to scan the wavelength range and confirm by transient spectroscopy the existence of the isosbestic points at 545 and 640 nm. As the monitoring wavelength was scanned down from 740 to 640 nm, the observed transient absorption kinetic trace was seen to decrease in intensity and become nonexistent around 640 nm. Between 640 and 540 nm, a transient bleach was observed of lower intensity than the corresponding maximum transient absorption. Below 545 nm a transient absorption was again observed. In essence, the scanning of the monitoring wavelength gives an indication of the optical absorption spectrum of the excited state; this spectrum corresponds to that obtained at 338 K. The observation of single exponential kinetics and isosbestic points in static and time-resolved spectroscopy is strong evidence that we have only two species present in equilibrium and that photoexcitation is effectively producing the hs-[$Co^{II}(SQ)_2$(N⌒N)] state which decays directly to the ls-[Co^{III}(SQ)(CAT)(N⌒N)] state.

Table 2. Variable Temperature Kinetic Parameters for the hs-[$Co^{II}(SQ)_2$(N⌒N)] to ls-[Co^{III}(SQ)(CAT)(N⌒N)] Valence Tautomeric Interconversion Determined by Means of Nanosecond and Picosecond Time-Resolved Optical Spectroscopy

complex	solvent	T [K]	K_{eq}	τ_{obs} [ns]	$10^{-6}k_{bvt}$ [s^{-1}]	$10^{-6}k_{fvt}$ [s^{-1}]
1	toluene	190.4	0.064	586	1.60	0.110
		200.2	0.149	434	2.01	0.294
		209.9	0.321	262	2.89	0.927
		219.5	0.647	181	3.36	2.17
		228.1	1.22	93.5	4.81	5.89
2	toluene	150.8	0	535	1.87	0
		161.4	0	294	3.40	0
		167.8	0	242	4.13	0
		180.9	0	169	5.92	0
		190.6	0.001	150	6.66	0.00667
		200.3	0.003	114	8.75	0.0230
		210.0	0.007	102	9.74	0.0680
		221.0	0.018	81.0	12.1	0.225
		230.0	0.045	66.2	14.5	0.655
		239.8	0.099	54.2	16.8	1.67
		249.8	0.205	40.6	20.4	4.19
3	toluene	181.0	0	409	2.45	0
		190.6	0	267	3.75	0
		200.8	0.001	187	5.34	0.00571
		211.1	0.003	120	8.31	0.0277
		220.5	0.008	86.6	11.5	0.0926
		230.0	0.019	62.7	15.7	0.300
		239.6	0.044	47.8	20.0	0.880
		249.0	0.094	35.0	26.1	2.46
		300.0	1.35	7.0	60.8	82.1
4	toluene	153.3	0	72.9	13.7	0
		161.3	0	50.6	19.8	0
		168.4	0	28.3	35.3	0
		181.0	0	20.6	48.0	0
		194.4	0	11.1	90.1	0
		298.0	0.24	1.2	671	162
4	2-methyltetra-hydrofuran	110.5	0	752	1.33	0
		120.9	0	594	1.68	0
		131.6	0	400	2.50	0
		143.3	0	194	5.16	0
		151.0	0	132	7.57	0
		161.3	0	67.3	14.9	0
		171.0	0	40.0	25.0	0
		181.0	0	27.3	36.7	0
		198.1	0	14.2	70.7	0

Arrhenius Behavior of the Rates of Valence Tautomeric Interconversion. Relaxation rates were determined for ~5 × 10^{-4} M toluene solutions of complexes **1**−**4** in the temperature range of 150−300 K. The results are tabulated in Table 2. Figure 13 shows the resulting hs- [$Co^{II}(SQ)_2$(N⌒N)] to ls-[Co^{III}-(SQ)(CAT)(N⌒N)] relaxation rate constants plotted as ln(k_{bvt}) versus 1/T. The relaxation process in this temperature regime is thermally activated, and the experimental data are well represented as a straight line. The results of fitting the relaxation data to the Arrhenius law given in eq 13 are plotted as solid lines. As summarized in Table 1, the activation energies E_a

$$k_{bvt} = Ae^{-E_a/kT} \tag{13}$$

for complexes **1**−**4** are 858, 582, 1088, and 856 cm^{-1}, respectively. There is no obvious correlation between the

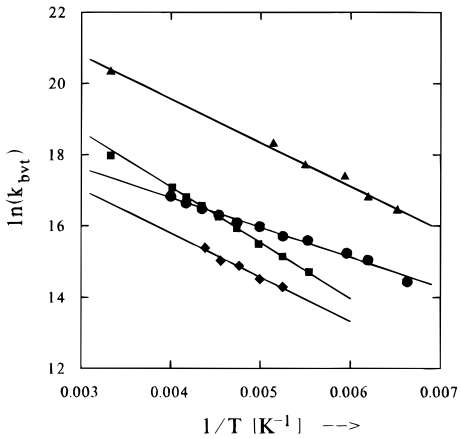

Figure 13. Observed hs-[$Co^{II}(SQ)_2$(N⁀N)] to ls-[Co^{III}(SQ)CAT)-(N⁀N)] relaxation rates plotted as ln(k_{bvt}) versus 1/T for complexes **1**−**4** in toluene solution: (◆) [Co(3,5-DTBSQ)$_2$(phen)] (**1**); (●) [Co-(3,5-DTBSQ)$_2$(bpy)] (**2**); (■) [Co(3,5-DTBSQ)$_2$(dmbpy)] (**3**); and (△) [Co(3,5-DTBSQ)$_2$(dpbpy)] (**4**). The solid lines represent fits of the data to the Arrhenius equation (eq 14).

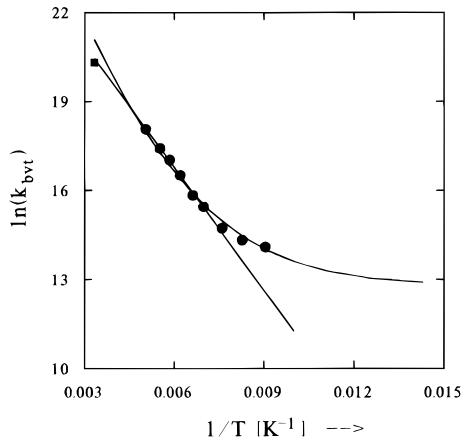

Figure 14. Observed hs-[$Co^{II}(SQ)_2$(N⁀N)] to ls-[Co^{III}(SQ)CAT)-(N⁀N)] relaxation rates plotted as ln(k_{bvt}) versus 1/T for complex **4** in 2-methyltetrahydrofuran. The straight solid line represents a fit of the data to the Arrhenius equation (eq 14). The curved solid line represents a fit of the data to the Jortner equation (eq 17).

activation energies and the energy separations ΔH listed in Table 1, however some inferences can be made. It is likely that the degree of electronic coupling varies among this series of valence tautomeric complexes, and consequently, this impacts on the apparent barrier height. The preexponential factors for complexes **1** and **2** are of similar magnitude. The critical temperature for complex **2** is shifted by ∼50° to higher temperature which is a reflection of the increased energy separation (ΔH) between valence tautomeric forms for this complex compared to that for complex **1**. The apparent decrease in activation energy from 858 to 582 cm^{-1} observed for complexes **1** and **2**, respectively, likely reflects the decreased barrier height due to the increased energy separation. Complexes **3** and **4** exhibit rather different preexponential factors and their barrier heights and energy separations do not allow for a simple interpretation. One notable general trend, however, is that the rate of k_{bvt} in the high temperature limit seems to increase as the critical temperature increases (i.e., k_{bvt} above 220 K falls in the order of complex **1** < complex **2** < complex **3** < complex **4**, where $T_{1/2}$ increases in the order of 226.6, 277.0, 286.6, 350.0 K, respectively).

In order to observe deviations from Arrenhius behavior, it is necessary to investigate the dynamics at temperatures below ∼140 K. The use of toluene as solvent precluded such an investigation since toluene tends to become optically opaque below temperatures of ∼150 K. It was for this reason that the dynamics of complex **4** were investigated in 2-methyltetrahydrofuran(MTHF), which forms a much more transparent glass at low temperatures. The variable temperature rate constants for back valence tautomerization of a 5×10^{-4} M solution of complex **4** in MTHF are listed in Table 2. The observed rates in the 150−200 K range are similar to those observed in toluene. Figure 14 shows the resulting hs-[$Co^{II}(SQ)_2$(dpbpy)] to ls-[Co^{III}-(SQ)(CAT)(dpbpy)] relaxation rate constants plotted as ln(k_{bvt}) versus 1/T. It can be seen that at temperatures above 140 K the hs-Co^{II} to ls-Co^{III} interconversion is a thermally activated process. However, at temperatures below 140 K, deviations from linearity are observed. The straight line represents a fit of the data in the 150−200 K to eq 14, where E_a is found to be 959 cm^{-1} and ln A is 25.05. Ferrous spin crossover complexes show deviations from Arrhenius behavior at temperatures below ∼120 K, where the relaxation rate becomes temperature independent as $T \rightarrow 0$. This behavior has been ascribed to a tunneling process. The above data seem to suggest that the valence tautomeric interconversion likewise may involve a tunneling process.

Kinetic Control of the hs-Co^{II} to ls-Co^{III} Valence Tautomeric Relaxation. One important goal of this research was to elucidate the microscopic details of the mechanism of valence tautomerization process b in order to control the rate of valence tautomerization. The rate of interconversion from hs-[$Co^{II}(SQ)_2$] to ls-[Co^{III}(SQ)(CAT)] in these complexes will fundamentally be dictated by the extent of electronic coupling between initial and final states (H_{if}), the energy separations between tautomeric states (ΔE), the magnitude of the change in the reaction coordinate (ΔQ), and the vibrational modes which make up the reaction coordinate ($\hbar\omega$).

The hs-Co^{II} to ls-Co^{III} valence tautomeric interconversion is similar to the Fe^{II} spin crossover interconversion. The single most prominent geometry changes for Fe^{II} spin crossover and the valence tautomerism are the metal−ligand bond length change (Δr) of 0.16−0.22 Å. The cobalt complexes also present internal ligand geometry changes since an electron is transferred between the metal and ligand. Spin crossover and valence tautomerism can be thermally driven; the entropy gain is of the same order of magnitude and the energy separations between limiting forms lie in a similar range of 300−3000 cm^{-1}. The spin crossover relaxation process is thermally activated at elevated temperatures but at temperatures below ∼140 K deviates from simple Arrhenius behavior and becomes temperature independent. This behavior is typical of a tunneling process. Likewise, the valence tautomeric process is thermally activated at high temperature, displaying similar activation energies (E_a) and preexponential factors (A) to Fe^{II} spin crossover complexes.[17] Furthermore, the valence tautomeric relaxation begins to show deviations from Arrhenius behavior at ∼140 K. Moreover, the observed relaxation rates of spin crossover and valence tautomerism are similar to within an order of magnitude.

Important work has elucidated some of the factors which modulate the rate of the Fe^{II} spin crossover interconversion.[17] The large geometric changes, the energy separations, and the small values of the electronic coupling in spin crossover complexes have been shown to be key factors that modulate the rate of spin crossover relaxation. The rates of high-spin → low-spin crossover in solution at room temperature for Fe^{II} complexes are of the order of 10^6-10^8 s^{-1}. For the four cobalt valence tautomeric complexes studied, the observed room-temperature rates of back valence tautomerization are found to

be in the range 10^7-10^8 s^{-1}. Since the geometric changes and energy separations in these valence tautomeric complexes are of similar magnitude and nature to Fe^{II} spin crossover complexes, it seems likely that the electronic coupling is of comparable magnitude. However, the small electronic coupling in these valence tautomeric complexes probably results from a fundamentally different origin. The electronic coupling between two states can conveniently be described by the electronic coupling matrix element $H_{if} = \langle\Psi_f|H|\Psi_i\rangle$, where Ψ_i and Ψ_f correspond to the total electronic wave functions of the initial and final states and H is the total electronic Hamiltonian. Symmetry and spin restrictions are important factors in the evaluation of the extent of electronic coupling. The magnitude of H_{if} depends on the spin multiplicity differences between initial and final states, the symmetry of the donor and acceptor orbitals of the initial and final electronic states, and the availability of electronic states that can mix with the donor and acceptor wavefunctions. The magnitude of H_{if} in Fe^{II} spin crossover complexes is small since the $^5T_2$ to $^1A_1$ spin crossover involves a $\Delta S = 2$ transition that is formally spin forbidden and to first-order $H_{if} = 0$ (i.e., the $^5T_2$ and $^1A_1$ states are orthogonal). For Fe^{II} spin crossover complexes, the magnitude of H_{if} is dictated by a second-order spin−orbit interaction through the intermediacy of a $^3T_1$ state.

Magnetic exchange coupling in the cobalt valence tautomeric complexes allows for a $\Delta S = 0$ interconversion pathway and thus is formally spin allowed. The hs-Co^{II} complex is a magnetic-exchanged coupled system having one $S = {}^5/_2$, one $S = {}^1/_2$, and two $S = {}^3/_2$ states in close energy proximity. The ls-Co^{III} tautomer is an $S = {}^1/_2$ complex. The spin-allowed valence tautomeric interconversion likely involves the $S = {}^1/_2$ state of the hs-Co^{II} tautomer. The electronic structures of the $S = {}^1/_2$ valence tautomeric states are shown in Figure 7. The cobalt valence tautomeric system is fundamentally a linked donor−acceptor electron transfer system, where the molecular orbital symmetries of the donor and acceptor moieties are expected to influence the magnitude of H_{if}. The valence tautomeric interconversion from hs-[$Co^{II}(SQ)_2$] to ls-[Co^{III}(SQ)(CAT)] is an intramolecular electron transfer process and involves the initial transfer of an electron from the highest occupied hs-Co^{II} e_g* donor orbital to the unoccupied π*-acceptor orbitals of the semiquinone ligands. Theoretical investigations of electronic coupling in electron transfer systems have shown that the magnitude of electronic coupling H_{if} depends on the matrix element $\langle\psi_i|\psi_f\rangle$, where ψ_i and ψ_f are the molecular orbitals of the initial and final state which donate and accept the electron, respectively.[33] Density functional LCAO electronic structure calculations of cobalt valence tautomeric complexes have shown the donor and acceptor orbitals to be orthogonal to each other, and mixing has been shown to be negligible. Consequently, H_{if} is not expected to be large. Such orbital symmetry restrictions have been shown to retard the rate of intramolecular electron transfer in linked $Ru^{II}-Co^{III}$ complexes.[18] In summary, the tunneling matrix element H_{if} is small for cobalt valence tautomeric complexes due to poor orbital overlap, whereas H_{if} is small in Fe^{II} spin crossover complexes due to spin restrictions.

Another electron transfer system that has some similarities to the valence tautomeric system is the self-exchange electron transfer reaction of hexaamminecobalt complexes in solution shown in eq 14:

$$\text{hs-}[Co^{II}(NH_3)_6]^{2+} + \text{ls-}[Co^{III}(NH_3)_6]^{3+} \underset{k_{-1}}{\overset{k_1}{\rightleftharpoons}} \text{ls-}[Co^{III}(NH_3)_6]^{3+} + \text{hs-}[Co^{II}(NH_3)_6]^{2+} \quad (14)$$

The study of this electron exchange has proved to be a long-standing problem in coordination chemistry.[34] The rate of electron transfer between the cobalt ammine complexes has been observed to be remarkably slow relative to analogous self-exchange couples of other transition metal complexes such as Fe^{II}/Fe^{III} and Ru^{II}/Ru^{III}. In fact, relative to the hexammineruthenium complexes, the bimolecular rate of electron transfer for the above cobalt complexes is $\sim 10^{13}$ times slower at room temperature. The most obvious difference between the Co^{II}/Co^{III} systems and those of Fe^{II}/Fe^{III} and Ru^{II}/Ru^{III} is that the former requires change in the spin state at the cobalt ions. The electronic configurations of the interacting species in the cobalt self exchange system are

$$(t_{2g})^6(e_g^*)^0 + (t_{2g})^5(e_g^*)^2 \rightleftharpoons (t_{2g})^5(e_g^*)^2 + (t_{2g})^6(e_g^*)^0 \quad (15)$$

The electronic structure change in this electron transfer system is fundamentally similar to the electronic structural change of the valence tautomeric interconversion shown in Figure 7. Since both reactions involve a change in two e_g* electrons, the metal−ligand bond length changes are both $\sim$0.18 Å. The electron transfer process in both cases involves interconversion between ls-Co^{III} and hs-Co^{II}. The self-exchange reaction is a $\Delta S = {}^3/_2$ process and is formally spin forbidden whereas the electron transfer is between e_g* orbitals and is orbitally allowed. Calculations have shown that the retardation of the self-exchange rate in hexamminecobalt complexes is due mainly to geometrical reorganization energies (10^8) associated with the large metal−ligand bond length changes and to a lesser extent to the spin multiplicity restrictions (10^4).[35]

Theoretical Analysis of Temperature Dependence of Rates of Tautomerism. In order to elucidate the microscopic details of the mechanism of valence tautomerization process b, it is necessary to place the valence tautomeric process within some theoretical framework. A quantum mechanical theory of radiationless transitions was proposed by Buhks and Jortner et al. in order to explain the dynamics of spin crossover processes in solution.[20] In this model, the *hs* → *ls* relaxation is described as a non-adiabatic radiationless process in the strong vibronic coupling limit occurring between two spin states in different nuclear configurations. In this theory, the electronic energy of the initial state is transformed into the vibrational energy of the final state. The theory has been successfully applied to the Fe^{II} spin crossover relaxation in polymer films,[36] solution,[37] pure solid compounds, and dilute mixed crystals.[12,17] Important parameters which modulate the rate of relaxation such as ΔE, H_{if}, $\hbar\omega$, and ΔQ are likely similar to those for the valence tautomeric process, and it is reasonable to describe the valence tautomeric interconversion within the framework proposed by Buhks and Jortner et al.

The conversion between the ls-Co^{III} and hs-Co^{II} states can be described in terms of a one-dimensional potential energy diagram (Figure 15). The simplest model for treating the valence tautomeric interconversion is the single configurational

(33) (a) Koga, N.; Sameshima, K.; Morokuma, K. *J. Phys. Chem.* **1993**, *97*, 13117. (b) Sanz, J. F.; Malrieu, J. P. *J. Phys. Chem.* **1993**, *97*, 99. (c) Newton, M. D. *Chem. Rev.* **1991**, *91*, 767.

(34) Newton, M. D. *J. Phys. Chem.* **1991**, *95*, 30.

(35) Buhks, E.; Bixon, M.; Jortner, J.; Navon, G. *Inorg. Chem.* **1979**, *18*, 2014.

(36) Xie, C. L.; Hendrickson, D. N. *J. Am. Chem. Soc.* **1987**, *109*, 6981.

(37) Conti, A. J.; Xie, C. L.; Hendrickson, D. N. *J. Am. Chem. Soc.* **1989**, *111*, 1171.

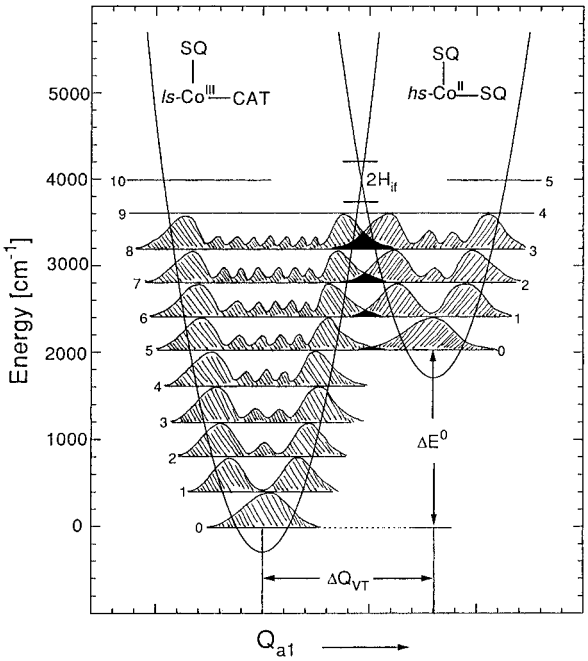

Figure 15. Quantum mechanical potential energy diagram for the ls-Co^{III} and hs-Co^{II} valence tautomeric states, plotted along the totally symmetric normal coordinate Q with $\Delta Q = \sqrt{6}\,\Delta r$. In the simple SCC model, harmonic potentials with equal force constants are used. The vibrational energy levels are shown with the squares of the vibrational wave functions superimposed.

coordinate (SCC) model where the reaction coordinate follows a certain nuclear coordinate. Since the largest geometric changes which accompany the valence tautomeric process are the metal−ligand bond lengths where Δr is ∼0.18 Å, an initial assumption is that the reaction coordinate will be approximately equivalent to the totally symmetric stretching normal coordinate of the complex, where $\Delta Q = \sqrt{6}\Delta r$. The rate at which the hs-Co^{II} state converts to the ls-Co^{III} state depends on the magnitude of the change in the reaction coordinate (ΔQ), the frequency of the active metal−ligand vibrational mode ($\hbar\omega$), the energy difference (ΔE), and the magnitude of the electronic coupling between the initial and final states (H_{if}).

Starting from the Fermi golden rule and invoking the Condon approximation Buhks and Jortner et al. derived the following rate expression for radiationless spin conversion processes in solution:

$$k = (2\pi/\hbar)g_f|H_{if}|^2G \tag{16}$$

The parameter g_f is the electronic degeneracy of the final state (i.e., $g_{hs-Co^{II}} = 16$ and $g_{ls-Co^{III}} = 4$). The Condon approximation assumes that the electronic matrix element in the region of the curve crossings is sufficiently constant and can be factored out of the total matrix element (separable nuclear and electronic wave functions) leaving the nuclear part in the factor *G*. The thermally averaged Franck−Condon nuclear vibrational overlap factor *G* accounts for the contribution of solvent and metal−ligand vibrational modes. In order to arrive at an analytical expression for *G*, a relatively simple model of the vibrational mode was assumed. The solvent is represented by very low frequency oscillators, and it is assumed that the initial and final states are approximated as harmonic potentials with equal force constants *f* and that a single metal−ligand vibrational mode $\hbar\omega$ is coupled to the interconversion.

Figure 15 presents the salient features of the theory in graphical form. Initially, the system is in the hs-Co^{II} state and contains a Boltzmann population of oscillators all of which have the frequency ω. These oscillators can exist in quantum states whose energies are given by $E_n = (n + {}^1/_2)\hbar\omega$. In Figure 15, superimposed on each vibrational level is drawn the square of the vibrational wave function for that level. The complex tunnels from the hs-Co^{II} state to the ls-Co^{III}, where the electronic energy of the hs-Co^{II} state is transformed into the vibrational energy of the ls-Co^{III} state. The vibrational energy is then dissipated by heat while the ls-Co^{III} complex settles to a new thermal equilibrium. The probability of the interconversion, and conseqently, the rate of the process is dependent on the magnitude of the electronic coupling and the square of the overlap integral [$C(n, n + p)$] of the vibrational wave functions given by

$$C(n, n+p) = \int \chi_n \chi_{n+p}\, dx = \langle \chi_n | \chi_{n+p} \rangle \tag{17}$$

where χ_n is the vibrational wavefunction for the *n*th vibrational level in the hs-Co^{II} state, χ_{n+p} is the wave function in the ls-Co^{III} state, and *x* is the oscillator coordinate. The absolute value of $C^2(n, n + p)$ is the Franck−Condon factor. The factor $C^2(n, n + p)$ is qualitatvely represented in Figure 15 as the shaded areas of overlap. The thermally averaged Franck-Condon factor is then given by

$$G(T) = \frac{\sum_n |(\chi_n|\chi_{n+p})|^2 e^{-n\hbar\omega/kT}}{\sum_n e^{-n\hbar\omega/kT}} \tag{18}$$

where the sum is over all vibrational levels *n* of the initial hs-Co^{II} state. As $T \rightarrow 0$, only the lowest energy vibrational level will be populated and the theory predicts a temperature-independent rate at low temperature.

In fitting the valence tautomeric rate constant data to the expanded version of eq 16 given explicitly in ref 20, the parameters include H_{if}, $\hbar\omega$, *p*, and *S*. The parameters of $\hbar\omega$, *p*, and *S* are part of the nuclear vibrational overlap factor *G* derived by Buhks and Jortner et al. The one active metal−ligand vibrational mode is characterized by $\hbar\omega$, and *p* is simply the reduced energy gap which for the analytical expression is necessarily an integer value.

$$p = \Delta E^0/\hbar\omega \tag{19}$$

The energy gap ΔE is a measure of the vertical displacement of the two potential wells relative to each other. The parameter *S* is the Huang−Rhys factor and measures the contribution of the change in the metal ligand vibrational mode,

$$S = m\omega(\Delta r)^2/2h = {}^1/_2 f\Delta Q^2/\hbar\omega \tag{20}$$

where *m* is the reduced mass and *f* is the force constant. *S* measures the horizontal displacement of the two potential wells and is related to the reorganization energy (λ) by $S = \lambda/\hbar\omega$. For Fe^{II} complexes with a [FeN_6] core, the value for *S* of 40−50 has been estimated from a $\Delta r_{HL} = 0.16$−0.22 Å, a mean force constant of $f \approx 2 \times 10^5$ dyn/cm, and a typical vibrational frequency of 200−300 cm^{-1}.[17] Experimental values for *S*, obtained from fitting experimental rate data to eq 16, tend to give values which range from 18 to 28.[36,37] The cobalt valence tautomeric complexes have a [CoN_2O_4] coordination, and estimation of *S* is not as straightforward. However, using an average value for Δr of 0.18 Å and a larger vibrational frequency of 350−450 cm^{-1} together with a larger force constant, a value for *S* of 30−40 can be estimated.

Table 3. Parameters Obtained from the Fit of the Relaxation Rate Data to the Jortner Equation (eq 16)[a]

complex	H_{if} [cm^{-1}]	$\hbar\omega$ [cm^{-1}]	S	ΔE [cm^{-1}]	p
1 phen	7.00	389	29.0	2336	6
2 bpy	5.38	389	29.0	3115	8
3 dmbpy	35.6	357	39.3	3216	9
4 dpbpy	88.0	334	32.1	1669	5

[a] See text for the definition of the parameters H_{if}, $\hbar\omega$, S, ΔE, and p.

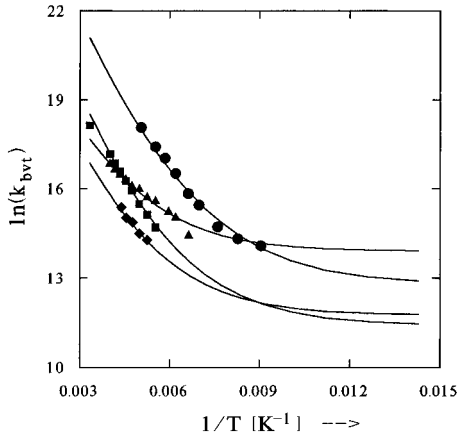

Figure 16. Observed hs-[Co^{II}(SQ)$_2$(N⌒N)] to ls-[Co^{III}(SQ)CAT)-(N⌒N)] relaxation rates plotted as ln(k_{bvt}) versus 1/T for complexes **1**−**4**: (◆) [Co(3,5-DTBSQ)$_2$(phen)] (**1**) in toluene; (△) [Co(3,5-DTBSQ)$_2$(bpy)] (**2**) in toluene; (■) [Co(3,5-DTBSQ)$_2$(dmbpy)] (**3**) in toluene; and (●) [Co(3,5-DTBSQ)$_2$(dpbpy)] (**4**) in MTHF. The solid lines represent fits of the data to the Jortner equation (eq 16).

In the least-squares fitting of the rate data to eq 16, the values of ΔE ($\sim\Delta H$) from solution magnetic susceptibility were used and held constant. We could only employ integer values of p since the analytical expression involves modified Bessel functions. Consequently the values of ΔE are slightly different from those obtained from the magnetic data. Table 3 lists the parameters obtained from the best fits of the rate data for the four cobalt complexes. The plots of data and the fits are displayed in Figure 16. As expected from theory the process is thermally activated at higher temperatures and becomes temperature independent as T $\rightarrow$ 0. The values of H_{if} obtained in the fitting range from 5.38 to 88 cm^{-1}; these values are consistent with two weakly interacting states. The quantum for the single active vibrational mode of $\hbar\omega$ was found to range from 334 to 389 cm^{-1}, which is consistent with a M−L stretching frequency. Moreover, the value of S was found to range from 29.0 to 39.3, which is consistent with the observed metal−ligand bond length changes. Reasonable fits could be obtained with only slight variations of the above parameters. Such slight variations mainly produced modifications in the low-temperature tunneling rates. In order to obtain better defined values for the above parameters, it is necessary to obtain the rate of back valence tautomerism as the temperature is decreased to liquid helium temperatures.

Concluding Comments

Data were presented to show that a series of four cobalt complexes undergo a valence tautomeric transformation from low-spin-[Co^{III}(SQ)(CAT)(N⌒N)] at low temperatures to high-spin-[Co^{II}(SQ)$_2$(N⌒N)] at high temperatures. Variable temperature magnetic susceptibility data for toluene solutions of the complexes were analyzed to evaluate ΔH and ΔS values characterizing the valence tautomeric equilibrium. The main conclusion is that the valence tautomeric transformation is entropy driven. The hs-Co^{II} tautomer has not only a greater electronic entropy but also a greater vibrational entropy than the ls-Co^{III} tautomer. The effect of the diiminium ligandN⌒N on the energy difference ($\Delta E \simeq \Delta H$) between the two tautomers was discussed in the context of a molecular orbital diagram.

The kinetics of the valence tautomeric interconversion (i.e., both forward and backward rates of hs-Co^{II} to ls-Co^{III} interconversion) were characterized by picosecond and nanosecond laser photolysis studies. When the complex is in the ls-Co^{III} form, it can be excited by a laser pulse to a LMCT excited state. Rapid intersystem crossing to the hs-Co^{II} state ensues, then allowing the determination of the rate of hs-Co^{II} to ls-Co^{III} conversion, k_{bvt}. At room temperature, k_{bvt} ranges from 6.1×10^7 to 6.7×10^8 s^{-1} for complexes **3** and **4** in toluene. The temperature dependence of k_{bvt} is Arrhenius-like in the 140−300 K range, but below ~140 K, deviations from linearity are seen. It is suggested that the valence tautomeric conversion involves quantum mechanical tunneling. The relatively slow rate of hs-Co^{II} to ls-Co^{III} conversion is attributable to poor overlap between donor and acceptor molecular orbitals. This is in contrast to the relatively slow rates of spin state interconversion of Fe^{II} spin crossover complexes that reflect a $\Delta S = 2$ spin-forbidden transition.

Acknowledgment. This work was supported by NSF grant CHE-9420322 (D.N.H.).

Supporting Information Available: Figures S1−S4 showing variable temperature magnetic susceptibility data (χT vs T) for all complexes and electronic spectra for complexes **2** and **3** in toluene and for complex **3** at 298 K in polystyrene (5 pages). See any current masthead page for ordering and Internet access instructions.

JA9619566